JOURNAL OF GEOPHYSICAL RESEARCH, VOL. 95, NO. B6, PAGES 9153-9170, JUNE 10, 1990

Densities and Porosities in the Oceanic Crust and Their Variations With Depth and Age

R. L. CARLSON AND C. N. HERRICK

Geodynamics Research Institute and Department of Geophysics, Texas A&M University, College Station

We have used drilling and downhole logging results (from Deep Sea Drilling Project holes 395A and 418A), measured properties of core samples from the seafloor and from ophiolites, and seismic velocity structure models of the oceanic crust to constrain empirical (statistical) relationships between in situ densities, porosities, and seismic velocities and to estimate densities and porosities in the oceanic crust, with the following principal results. Our review of drilling results and studies of ophiolites suggests that the velocity structure of the oceanic crust is more closely related to changes in porosity and alteration (or metamorphic grade) than to its igneous structure: the transition from layer 2a (3.7 ± 0.4 km s^{-1}) to 2b (5.2 ± 0.4 km s^{-1}) occurs within the extrusive pile; the top of layer 2c ($6.2 + 0.2$ km s^{-1}) is associated with the top of the sheeted dike complex and with the first appearance of greenschist facies alteration products; ophiolite studies have shown that the top of layer 3 occurs within the sheeted dikes where the metamorphic grade of alteration products increases from greenschist to amphibolite facies. A comparison of reprocessed and corrected downhole logs from holes 395A and 418A indicates that in situ densities and fractional porosities differ by 0.2 Mg m^{-3} and 0.07, respectively. These differences are consistent with prevailing views of the progressive alteration of the upper oceanic crust. Statistical relationships between in situ density, porosity and slowness are highly linear, and indicate that the density/slowness relation estimated from laboratory samples [$\rho_b = (3.81 \pm 0.02) - (6.0 \pm 0.1)S$] applies to in situ properties as well. We obtained a similar empirical relationship for porosities from the hole 418A log data [$\Phi_f = -(0.35 \pm 0.03) + (2.37 \pm 0.15)$ S; $r^2 = 0.84$ S.E. = 0.015]. Applying these empirical models to seismic velocity structure models yields the following crustal densities and porosities: layer 2, 2.62 - 2.69 Mg m^{-3}, 0.10 - 0.12 and layer 3, 2.92 - 2.97 Mg m^{-3}. The estimated average density of the oceanic crust is 2.86 ± 0.03 Mg m^{-3}. Densities and porosities estimated from a seismic crustal structure model for old Atlantic crust agree very well with the logging data from hole 418A, suggesting that in situ densities and porosities can be estimated from seismic velocities. High density and porosity gradients are characteristic of the upper oceanic crust; increasing densities reflect both a progressive decrease of porosity and increasing grain density with depth. Based on the seismic properties of layer 2a, we estimate that the layer thins at an approximate rate 20 to 45 m m.y.$^{-1}$ while the velocity increases by 0.040 km s^{-1} m.y.$^{-1}$. The corresponding rates of change of density and porosity are 0.016 ± 0.009 Mg m^{-3} m.y.$^{-1}$ and -0.005 ± 0.003 m.y.$^{-1}$, respectively.

1. Introduction

Numerous marine geological and geophysical studies have the objectives of ascertaining the structure, composition and physical state of the oceanic crust and their dependence on age. Two of the most important state parameters are density and porosity, which have important implications for a host of problems. Among them are the progressive alteration of the crust by hydrothermal circulation in the first few million years after its formation, interpretations of marine gravity data, the variation of lithospheric buoyancy with age, and the role and fate of the crust in subduction or subduction-related processes. In the absence of a systematic estimate of crustal density various investigators have used values ranging from 2.7 to 3.0 Mg m^{-3} [*Watts and Talwani*, 1974; *Oxburgh and Parmentier*, 1977; *Molnar and Atwater*, 1978; *Pennington*, 1983]; others have ignored the effect of the crust altogether.

In their study of the velocity structure of the Bay of Islands ophiolite, *Salisbury and Christensen* [1978] noted that the densities of hand samples range from 2.85 Mg m^{-3} near the top of the section to 2.98 Mg m^{-3} near the base of the gabbros, with an average of 2.91 Mg m^{-3}. *Christensen and Smewing* [1981] found similar values for the Semail ophiolite, but hand sample densities cannot be regarded as representative of in situ values owing to the large-scale porosity of oceanic layer 2 [e.g., *Hyndman and Drury*, 1976]. In situ densities and porosities can be measured only by downhole logging. Unfortunately, only hole 504B has penetrated the crystalline basement to a depth of more than 700 m [*CRUST*, 1982; *Cann et al.*, 1983; *Anderson et al.*, 1985a; *Becker et al.*, 1988] and only one deep hole in basement more than 10 m.y. old has been thoroughly investigated; hole 418A (110 Ma) was cored to a sub-basement depth of 544 m on Deep Sea Drilling Project (DSDP) legs 51-53 [*Donnelly et al.*, 1980] and logged on Ocean Drilling Program (ODP) leg 102 [*Salisbury et al.*, 1986]. Owing to the paucity in situ data, densities and porosities in the oceanic crust must be inferred largely from its seismic velocity structure.

Carlson and Raskin [1984] combined laboratory data, downhole logging results and seismic structure models to estimate crustal densities by three different methods. Their estimates of mean crustal density range from 2.86 to 2.89 Mg m^{-3}. While this difference is small, layer 2a densities estimated by the different methods differ by as much as 0.30 Mg m^{-3}. Further, much of the log data available to *Carlson and Raskin* [1984] was of poor quality and virtually all of the logs were from young sites (< 10 Ma). Thus, they could not show that the results apply to "typical" oceanic crust having an age of several tens of millions of years. The acquisition of a suite of high-quality logs from hole 418A [*Salisbury et al.*, 1986] offered an opportunity to evaluate the in situ density/velocity systematics of an old (110 Ma) upper crustal section. *Carlson et al.* [1988] estimated the average density of old (more typical) oceanic crust to be about 2.86 Mg m^{-3}. This value is within the range of the previous estimates. However, the properties of young oceanic crust remain problematical. Moreover, there has been no attempt to assess the porosity

Paper number 89JB03583.
0148-227/90/89JB-03583$05.00

structure of the oceanic crust, and the variations with age of density and porosity of the uppermost oceanic crust (layer 2a) have not been addressed.

This study has three primary objectives:

1. To establish porosity/density/velocity systematics based on downhole logging data from holes 395A (6 Ma) and 418A (110 Ma).

2. To evaluate the average density and porosity structures of the oceanic crust by applying the results to seismic velocity structure models, and

3. To evaluate the age dependence of the density and porosity of layer 2a based on the seismic data of *Houtz and Ewing* [1976].

The remainder of the paper is organized as follows: Section 2, seismic and lithologic structure of the oceanic crust; Section 3, summary of previous density studies; Section 4, analysis of downhole logs: holes 385A and 418A; Section 5, density, porosity, and velocity systematics; Section 6, density and porosity structure of the oceanic crust; Section 7, age dependence of layer 2a properties; and Section 8, summary and conclusions.

2. Seismic and Lithologic Structure of the Oceanic Crust

Most our our direct knowledge of oceanic crustal structure derives from seismic surveys; direct sampling is restricted to less than 700 m of basement penetration and the composition and structure of the bulk (80-90%) of the crustal section has been inferred largely by analogy with ophiolites. Numerous excellent reviews of seismic and lithostratigraphic structure have been published [e.g., *Christensen and Salisbury*, 1975; *Spudich and Orcutt*. 1980; *Lewis*, 1978; *Purdy and Ewing*, 1986], and much of the following is based on such summaries.

Prior to about 1970, numerous reconnaissance refraction surveys gave rise to classic three-layer models of the oceanic crust [*Raitt*, 1963; *Shor et al.*, 1971; *Christensen and Salisbury*, 1975]. Layer 2 was recognized as corresponding at least roughly with the extrusive pile which caps the basement section. Layer 3 came to be regarded as representing an underlaying gabbro complex which constitutes the bulk of the crust.

In the last two decades more sophisticated survey methods and inversion techniques have led to a much more refined view of seismic structure. New interpretations indicate that the uppermost 2-3 km of oceanic basement ("layer 2") is a region of very high velocity gradients, with P wave velocities ranging from < 4 km s^{-1} at the top of the interval to >6 km s^{-1} near the bottom. Based on a large number of air gun/sonobuoy surveys in the Atlantic and Pacific oceans, *Houtz and Ewing* [1976] recognized some stratification within layer 2 (layers 2a, 2b, 2c), though these regions may not be homogenous or separated by distinct boundaries. Of particular interest is the observation that velocities near the top of the section increase as the crust ages; layer 2a gradually disappears. *Purdy and Ewing* [1986] have noted that this change represents virtually the only well-established, age-dependent variation in oceanic crustal structure. "Layer 3" is typically about 5 km thick and is characterized by a restricted range of velocities (6.5-7 km s^{-1}) and velocity gradients less than 0.1 s^{-1} G.M. Purdy (personal communication, 1989) has suggested some variation of layer 3 seismic structure with age, but this possibility remains to be confirmed. The Moho is now viewed as a transition region up to 1 km or more in thickness, across which seismic velocities increase to about 8 km s^{-1}, typical of the upper mantle.

In the absence of direct sampling of the oceanic crust by drilling, ophiolites have served as the best available lithostratigraphic model of the oceanic crust since the mid-1970s. Though ophiolites typically exhibit island arc (as opposed to mid-ocean ridge basalt (MORB)) geochemical affinities, the model they provide has served well; most of the seismic characteristics of the crust can be explained by studies of ophiolites combined with the results of drilling in the upper kilometer of the crust itself (e.g., *Christensen*, 1978; *Salisbury and Christensen*, 1978; *Christensen and Smewing*, 1981; *Anderson et al.*, 1982; *Becker et al.*, 1988].

The principal lithologies present in ophiolites are basalts, diabases, gabbros, and their metamorphic equivalents. A much simplified sequence, viewed from the top downward, consists of 1-1.5 km of extrusive, generally pillowed, basalts, 1-1.5 km of sheeted diabase dikes, and a high-level isotropic gabbro sequence of variable thickness (up to 1 km), which grades downward to 3-to 5-km-thick sequence of mafic, layered gabbros (hornblende, pyroxene and olivine gabbros, troctolite), in which the ultramafic component typically increases with depth. The crustal section has been variably affected by hydrothermal alteration; the metamorphic grade of the alteration products generally increases (zeolite to greenschist to lower amphibolite facies), while the intensity of metamorphism decreases with depth. The layered gabbros are commonly interlayered with ultramafic rocks in the lowermost part of the "crustal" section, above the ultramafic "mantle."

The seismic structures of ophiolites, reconstructed from laboratory studies of ophiolite rocks, compare very favorably with the seismic structure of the oceanic crust [*Christensen*, 1978; *Salisbury and Christensen*, 1978; *Christensen and Smewing*, 1981; *Christensen and Salisbury*, 1982]. In ophiolites, "layer 2" is characterized by strong velocity gradients which extend well into the sheeted dikes and correlate with a systematic decrease of grain-boundary porosity and with and a systematic increase of metamorphic grade (zeolite to upper greenschist facies) with depth. Velocities typical of layer 3 are encountered in the mid to lower portions of the sheeted dike complex, where upper greenschist alteration assemblages give way to those of lower amphibolite grade. Velocity gradients below this level are low, and differences in the amount of modal olivine present in the layered gabbro sequence, and/or the intensity of metamorphism may account for slight variations of layer 3 velocity structure. The transition from "crustal" gabbros to "mantle" ultramafic rocks can be abrupt, but is commonly gradational, and velocity anisotropy in the ultramafic rocks [*Christensen and Salisbury*, 1979] closely approximates the pattern of seismic anisotropy observed in the oceanic upper mantle [e.g., *Morris et al.*, 1969].

Results of DSDP and ODP drilling and downhole measurements in oceanic basement are broadly consistent with the ophiolite model. Of several holes in which basement penetration is significant, only hole 504B has reached beyond the extrusive pile. The site is located 200 km south of the Costa Rica Rift (Figure 1) where the age of the basement rocks is 6 Ma. Drilling on DSDP legs 69, 70 and 83 and ODP leg 111 [*CRUST*, 1982; *Cann et al.*, 1983; *Anderson et al.*, 1982, 1985a; *Becker et al.*, 1988] has reached a sub-basement depth of nearly 1300 m, about 500 m into a sheeted dike complex. Numerous logging and downhole experiments have been conducted in the hole [e.g., *Anderson et al.*, 1982; *Becker et al.*, 1982, 1988]. As noted by *Becker at al.*, [1988, p. 36], "...the lithostratigraphy sampled in hole 504B is the best direct, if limited, verification of the ophiolite model of the oceanic crust..."

To a depth of about 570 msb (meters subbasement) the hole 504B section consists of pillow basalts with associated breccias, hyaloclastites and minor flows. The interval between 570 and 780 msb represents a transition zone in which pillows give way to sheeted dikes (evidenced by steeply dipping chilled margins) and massive basalt units. From 780 msb to the bottom of the hole (at 1287 msb) the section has been interpreted as a sheeted dike complex of the type so commonly observed in ophiolites.

The upper oceanic crust at site 504 has been hydrothermally altered [*Honnorez et al.*, 1985; *Alt et al.*, 1985, 1986]. The extrusive pile has been altered at temperatures generally less than 100°C; above about 320 msb the dominant alteration products are iron hydroxides, celadonite and saponite. Higher temperature phases (talc, saponite, zeolites, disseminated pyrite), formed at about 100° C, appear between 225 and 250 msb, and are the

dominant alteration products in the lower part of the extrusive pile. Greenschist facies alteration products (chlorite, epidote, actinolite) appear abruptly near 625 msb, and are characteristic of the dike complex to the bottom of the hole [*Alt et al.*, 1986; *Becker et al.*, 1988].

According to *Houtz and Ewing* [1976] seismic velocities characteristic of layers 2a, 2b, and 2c are, respectively, 3.6 ±0.4, 5.2 ±0.4 and 6.1 ±0.2 km s^{-1}. Intervals corresponding to layers 2a, 2b, and 2c can be recognized in hole 504B, albeit with some ambiguity. An oblique seismic experiment [*Little and Stephen*, 1985] failed to detect layer 2a but did indicate a high velocity gradient. Both the leg 83 sonic log [*Newmark et al.*, 1985] and a vertical seismic profile (VSP) conducted on leg 111 [*Becker et al.*, 1988] detected average velocities typical of layer 2a (3.7 km s^{-1}) in the upper 225 m of the section. Apparent porosities, derived from a large-scale resistivity experiment, [*Becker et al.*, 1982] decrease rapidly from near 0.14 to about 0.06 over this interval. The permeability is high, but decreases abruptly from > 10^{-14} m^2 to less than 10^{-6} m^2 near 225msb [*Anderson et al.*, 1982]. Layer 2a can thus be clearly associated with the uppermost alteration zone. The contact between layers 2a and 2b is marked by changes in permeability and in the dominant products of alteration.

Layer 2b extends downward into the transition zone. Conventional sonic logs [*Newmark et al.*, 1985], MCS logs and VSP data [*Becker et al.*, 1988] all show variable velocities having an average near 5.5 km s^{-1}, typical of layer 2b. Apparent porosities are also variable, ranging from 0.06 to 0.10 [*Becker et al.*, 1982], and the permeability is low, as noted above.

The 2b/2c contact is apparently transitional. Some investigators have located the top of layer 2c as deep as 900 msb, but MCS and VSP data [*Becker et al.*, 1988] indicate that velocities typical of layer 2c (6.1 ±0.2 km s^{-1}) are sustained below about 650 msb. Between 600 and 650 msb, apparent porosities decrease from near 0.08 to less than 0.03 [*Becker et al.*, 1982], pillow basalts give way to dikes, and greenschist facies alternation products first appear at about 625 msb. The transition from layer 2b to 2c is thus associated with an abrupt reduction in porosity, the onset of greenschist facies alteration and the top of the dikes, and cannot be clearly ascribed to a single effect. This ambiguity is perhaps to be expected.

Alt et al. [1986] have suggested that greenschist facies alteration reflects high-temperature hydrothermal circulation in the low-permeability dike rocks, whereas the upper part of the extrusive section was altered by seawater at low temperatures and the lower interval of the extrusive pile represents a region of high temperature gradients and mixed fluids. If this plausible model is correct, an association of the greenschist alteration assemblage with the top of the dike complex, and with the top of layer 2c would be expected.

In the context of crustal structure and composition, a site which must be mentioned is 735. Located on a tectonically unroofed and uplifted block at the Atlantis II Fracture Zone on the Southwest Indian Ridge [*Robinson et al.*, 1989], hole 735B penetrated 500 m of gabbro, olivine-gabbro and troctolite, with rare basalts and trondhjemites. A zone of very high density Fe-rich gabbros was penetrated between 225 and 275 msb. Observed foliated and mylonitized zones may have developed during the unroofing and emplacement of the block. Otherwise, the recovered gabbros are apparently quite similar to gabbros found in some ophiolites. The primary phases are pyroxene, plagioclase and olivine. The principal alteration product is green amphihole, but secondary minerals include tremolite, talc, pargasite, epidote, etc. Metamorphic grade is as high as upper amphibolite to granulite facies, and hydrothermal alteration was largely controlled by permeability. Laboratory samples have *P* wave velocities generally in the range 6.5-7.3 km s^{-1}, densities in the range 2.9-3.0 Mg m^{-3}, and porosities generally less than 1 percent. Sonic, VSP and MCS logs indicate that in situ velocities are slightly lower; 6.5 ±0.15 km s^{-1}. In situ densities are in the range 2.9-3.0 Mg m^{-3}. The original stratigraphic position of these gabbros is unknown, but the rocks described by *Robinson et al.* [1989] are most nearly analogous to the "isotropic" hornblende gabbros which underly the sheeted dikes at depths of 1.5 to 2 km in ophiolites, and the observed *P* wave velocities are consistent with this interpretation. Velocities near 6.5 km s^{-1} are also commonly observed at depths of 1.5 to 2 km in the oceanic crust [e.g., *Spudich and Orcutt*, 1980; *Purdy*, 1983; *Vera and Mutter*, 1988].

Of particular interest for this study are sites 395 and 418 (Figure 1). Located south of the Kane Fracture Zone and west of the Mid-Atlantic Ridge in crust about 6 Ma old, hole 395A was drilled

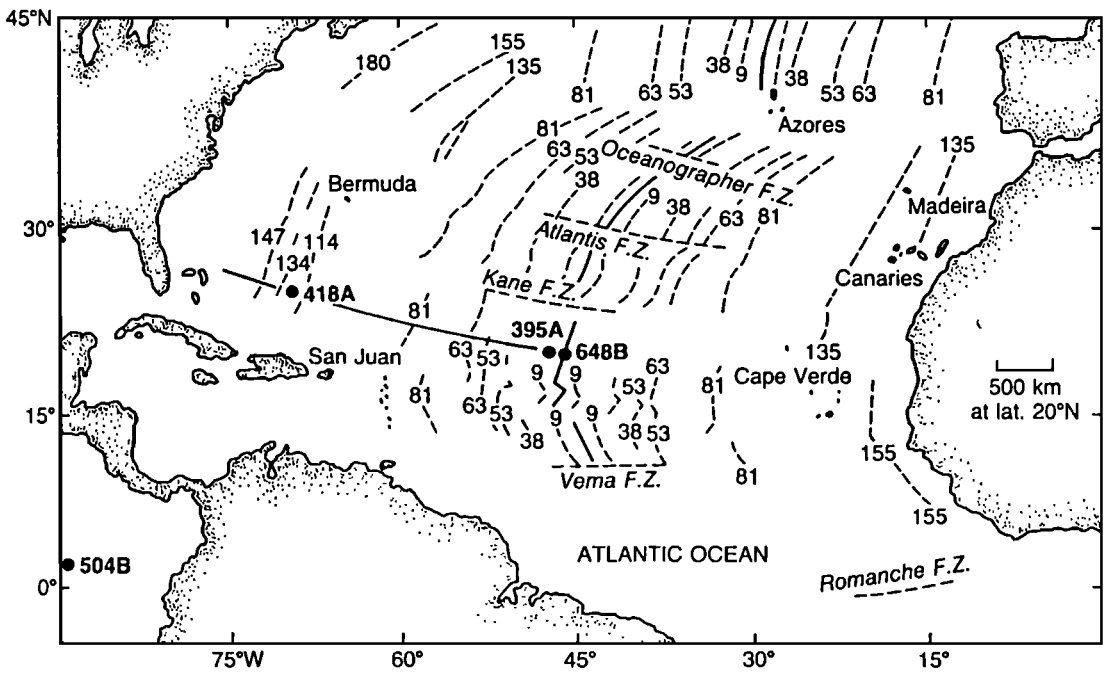

Fig. 1. Location map showing sites 395, 418 and 504 and 648 [*Bryan et al.*, 1988].

to a depth of about 570 msb on DSDP leg 45 [*Melson et al.*, 1979]. A comprehensive program of downhole logging and experiments was carried out on ODP leg 109 [*Bryan et al.*, 1988].

The dominant lithologies recovered from hole 395A are pillow basalts, minor massive flows and associated breccias and hyaloclastites [*Melson et al.*, 1979]. Evidence of low-temperature alteration is abundant: calcite veins are common, as are smectites (saponite) and zeolites. The only evidence of higher-temperature alteration is chlorite vesicle fillings in two massive flows and one intrusive unit.

Geophysical parameters are less easy to correlate with the drilling results from 395A than with those from 504B, partly because clear lithostratigraphic breaks are lacking and partly because the downhole logs from hole 395A are noisy owing to poor borehole conditions. Downhole logs suggest velocities less than 4 km s^{-1} in the upper part of the section, increasing to 5.0 to 5.5 near the bottom of the hole. Resistivity increases sharply at about 350 msb, and the permeability of the formation below about 300 msb is high [*Bryan et al.*, 1988]. These properties are consistent with the existence of layer 2a at this site.

Hole 418A (Figure 1), drilled during DSDP legs 51-53 [*Donnelly et al.*, 1980], penetrated 544 m into basement south of the Bermuda Rise where the age of the crust is 110 Ma. The hole was subsequently logged on ODP leg 102 to document the properties of the uppermost section of old crust [*Salisbury et al.*, 1986].

The 418A section represents an extrusive pile consisting of roughly 70% pillow basalts and 25% massive flows, with cemented basaltic breccias amounting to a few percent [*Salisbury et al.*, 1980]. The section is altered throughout. K_2O enrichment is characteristic, and the dominant alteration products are potassium feldspar, palagonite, smectite, calcite, and quartz. Zeolites are also present. Combined core and log analyses indicate that cracks and voids in the section have been largely filled or sealed by various alteration products [*Donnelly et al.*, 1980; *Salisbury et al.*, 1986, 1988 a, b].

In their exhaustive analysis of the downhole logs acquired on leg 102, *Broglia and Moos* [1988] recognized three distinct zones in the section. The top 64 m consists of comparatively unaltered pillow basalts having porosities less than 0.15 and velocities greater than 5 km s^{-1}, capped by a thin unit of more highly altered pillow basalts. The underlying unit, which extends from 64 to 190 msb, is an interval of extensively altered pillow basalts as evidenced by very high K_2O contents and consequent high levels of natural gamma radiation; fractures and voids contain large amounts of smectites. Sonic log velocities range from 3.5 to 5 km s^{-1}, and the smectite-corrected neutron log porosities range from 0.15 to 0.25. Below 190 msb, the degree of alteration is lower. Corrected porosities are less than 0.20, sonic velocities range from 4 to 6 km s^{-1}, and the smectite content is less than 5%. *Moos* [1988] reports that the average P wave velocity over the interval logged using the MCS tool (145 to 464 msb) is 5.5 km s^{-1}. Layer 2a is said to be absent at site 418.

In summary, seismic surveys, ophiolite studies and the results of coring and downhole logging in the uppermost part of the oceanic basement section lead to a broadly consistent picture of the structure of the oceanic crust. Layer 2 extends to a depth of 1.5 to 2.0 km and is composed largely of pillow basalts and a few massive flows. It is a region of very high velocity gradients; P wave velocitites range from less than 4 km s^{-1} at the top to more than 6 km s^{-1} at the bottom of the interval. The high velocity gradients have been attributed to a rapid decrease of both large-scale and grain boundary porosity with depth and to a corresponding increase in the metamorphic grade of alteration products. Velocities in the upper few hundred meters of the section increase with age owing to the progressive infilling and sealing of cracks and voids by alteration products. Layer 3 velocities are typically in the range 6.7 to 7 km s^{-1} and velocity gradients are low (less than 0.1 s^{-1}). To the extent that ophiolites are analogous to the oceanic crust, layer 3 may be said to consist largely of layered gabbros variably affected by amphibolite grade alteration, with an interval of isotropic gabbros and sheeted, diabase dikes near the top. Velocity variations within layer 3 may be attributed to changes in modal olivine content or alteration with depth. The oceanic Moho may be regarded as a transition zone up to 1 km or so in thickness, and consisting of interlayered gabbros and ultramafic rocks.

The seismic velocity structure of the oceanic crust is widely thought of as reflecting its igneous structure. However, in ophiolites velocities typical of layer 3 occur within the sheeted dike complex, with the first appearance of amphibolite grade alteration assemblages [*Christensen and Salisbury*, 1975; *Salisbury and Christensen*, 1978; *Spudich and Orcutt*, 1980]. In hole 504B, layer 2a correlates with an interval of high permeabilities and porosities and low-temperature alteration; layer 2b is an interval of lower porosities, markedly lower permeabilities and higher temperature alteration [*Becker et al.*, 1982; *Anderson et al.*, 1982, *Alt et al.* 1986]. Velocities typical of layer 2c are sustained below 600 to 650 msb. This interval correlates with the top of the sheeted dikes, the first appearance of greenschist facies alteration products and an abrupt reduction in porosity [*Becker et al.*, 1982; *Anderson et al.*, 1982; *Alt et al.*, 1986]. Taken together, these correlations suggest that the velocity structure of the oceanic crust is more indicative of variations of porosity and alteration (including metamorphic grade) than of its primary, igneous stratification.

3. Summary of Previous Density Studies

Previous estimates of the density structure of the oceanic crust have been made by *Carlson and Raskin* [1984] and *Carlson et al.* [1988], as noted above. Their methods and results are briefly reviewed in the following paragraphs.

These studies focused on the average density of the crustal section. To estimate the average density, *Carlson and Raskin* [1984] assumed that the oceanic crust may be regarded, on average, as a laterally homogenous medium. Any chosen property, say Θ then varies only with depth, and the average for the crust is simply

$$\bar{\Theta} = \frac{1}{H}\int_0^H \Theta(z)\,dz \tag{1a}$$

where H is the total thickness. In the discrete-layer case

$$\bar{\Theta} = \frac{1}{H}\Sigma \Theta_i h_i \quad H = \Sigma h_i \tag{1b}$$

where Θ_i and h_i represent the property and thickness of the i^{th} layer, respectively. Layer thickness can be taken directly from seismic structure models. The problem, as noted by *Carlson and Raskin* [1984], is one of estimating the corresponding layer properties. They used three different methods to estimate layer densities from eight average crustal structure models.

In the first case, Carlson and Raskin made a simple, qualitative correlation of ophiolite lithostratigraphy with the seismic structure of the oceanic crust. They then applied average densities of basalts, diabases, gabbros, metagabbros and olivine gabbros, in what they estimated to be appropriate combinations, to the structure models. Average crustal densities derived from the eight velocity structure models range from 2.89 to 2.91 Mg m^{-3}, with a mean of 2.90.

Carlson and Raskin also used density/velocity systematics to estimate layer densities from seismic structures. They found that the laboratory densities and velocities (measured at 40 MPa confining pressure) of rocks sampled from the seafloor and from ophiolites follow a simple linear relationship between density and slowness, as shown in Figure 2:

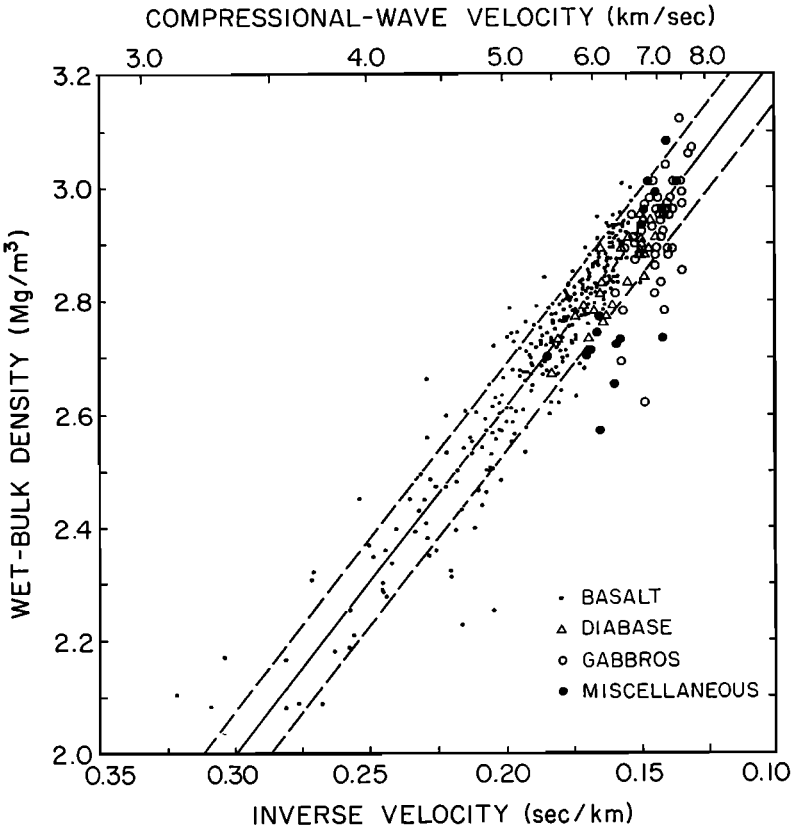

Fig. 2. Wet-bulk density versus P-wave slowness in laboratory samples from ophiolites and from the upper oceanic crust. Velocities were measured at 40 MPa confining pressure under water-saturated conditions. "Miscellaneous" includes rock types such as serpentinites and amphibolites which are present but not abundant in the oceanic crust. Solid line is best fit of density on slowness (equation (2a)); dashed lines represent rms error (see text and Table 2). [from *Carlson and Raskin*, 1984].

$$\bar{\rho} = (3.81 \pm 0.02) - (6.0 \pm 0.1)S \ (s\ km^{-1}) \qquad (2a)$$

with a coefficient of determination (r^2) of 0.86 and an rms error of 0.07 Mg m^{-3}. Applying this equation to the velocity-structure models produced mean crustal densities ranging from 2.84 to 2.90 with an average of 2.86 Mg m^{-3}. However, Carlson and Raskin also found that the average densities and slownesses obtained from downhole logs at a number of DSDP sites follow a markedly different "time-average" trend, (Figure 3):

$$\bar{\rho} = (3.5 \pm 0.2) - (3.8 \pm 0.1)S \qquad (2b)$$

The coefficients of equation (2b) were calculated from the properties of seawater (1.025 Mg m^{-3}, 1.5 km s^{-1}) and the statistically determined properties of zero-porosity, fresh basalt (2.93 ± 0.06 Mg m^{-3}, 6.65 ± 0.20 km s^{-1}). This equation was intended to account for the effects of large-scale porosity in layer 2 [e.g., *O'Connell and Budianski*, 1974; *Spudich and Orcutt* 1980]. Applying (2*b*) to the upper oceanic crust ($V_p < 6.65$ km s^{-1}) and (2*a*) to the deeper crust produced mean crustal densities ranging from 2.87 to 2.92, with an average of 2.89 Mg m^{-3}.

Because the uncertainties are in the range 0.02 to 0.06 Mg m^{-3}, the mean crustal densities estimated by these three methods are not statistically distinguishable. However, equations (2*a*) and (2*b*) yield appreciably different densities for layer 2; the estimated densities of layer 2a differ by as much as 0.30 Mg m^{-3}. The corresponding difference in in situ fractional porosity is about 0.15- a large fraction of the expected value representing a large systematic error. Further, the downhole log data shown in Figure

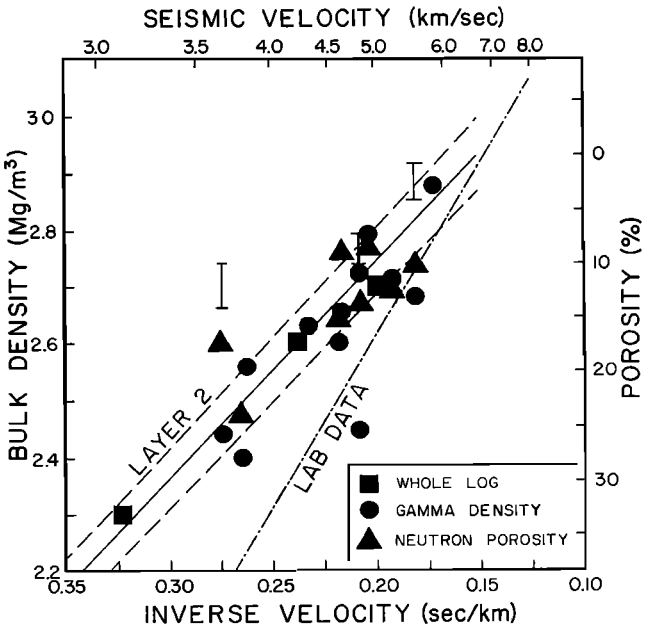

Fig. 3. Plot of in situ density and porosity vs. slowness from downhole logs at DSDP sites 395, 417, 504, 556, 558 and 564. Bars indicate apparent porosities from hole 504B. Solid line represents "time-average" relations for fresh basalt/seawater mixture; dashed line represents the error in the time-average equation. Dot-dash line shows best fit to laboratory data (see Figure 2). [from *Carlson and Raskin*, 1984].

3 are largely from holes in young oceanic crust, and are of notoriously poor quality [e.g. *Kirkpatrick*, 1979; *Cann and Von Herzon* , 1981]. Even if it is valid for young crust, equation (2*b*) cannot be said to apply to the oceanic crust in general.

For these reasons, *Carlson et al.* [1988] made a reevaluation based on downhole log data acquired from DSDP hole 418A on ODP leg 102 [*Salisbury et al.*, 1986, 1988a]. The log data from this hole are well-suited to the purpose for two reasons: Borehole conditions at 418A are excellent, so the raw log data are of good quality, and the Lamont Borehole Research Group [i.e., *Broglia and Moos*, 1988] took great pains to calibrate or correct the density and porosity logs.

Evaluating downhole logs from holes in oceanic basement is problematical. Conventional tools were designed for logging sediment sections and not for the poor borehole conditions or rock types of crystalline oceanic basement. Densities are measured indirectly by gamma ray attenuation. Where the roughness of the borehole wall prevents the tool from making good contact with the formation, densities are underestimated. The neutron porosity method is sensitive to the concentration of strong neutron absorbers. In geologic environments the primary absorber is hydrogen, in the form of pore water or in hydrous mineral phases (bound water). Where such phases are present, porosities are overestimated. Unfortunately, little is known about the neutron absorption characteristics of basaltic rocks and calibrating or correcting these logs is a difficult problem. Where borehole conditions are poor, sonic velocity measurements can be affected by noise (early arrivals) or missed first arrivals (cycle skipping). In the case of hole 418A, the sonic log data are of excellent quality [*Salisbury et al*, 1986, 1988a].

Broglia and Moos [1988] calibrated the density and porosity logs by assuming that the densities and porosities of core samples from massive flows are representative of the in situ values (i.e. that the massive units are not affected by large-scale porosity). They adjusted the logs by adding 0.04 Mg m^{-3} and -0.06 (-6 p.u.) to the log densities and porosities, respectively. *Broglia and Moos* also corrected the neutron porosities for smectite (bound water) content. The smectites recovered from hole 418A are unusual in that they contain large amounts of potassium, and the potassium concentration is reflected in the natural gamma log. By assuming that all of the potassium in the logged interval is associated with smectites, *Broglia and Moos* [1988] were able to estimate smectite volume fractions and hence to correct the neutron porosity logs.

Carlson et al. [1988] used the correct logs. Because much of the density data, particularly from the upper part of hole 418A, is of questionable validity, they also calculated densities from the corrected neutron porosities, assuming a grain density of 2.93 Mg m^{-3} and a pore fluid density of 1.025 Mg m^{-3}. They found that the in situ densities and slownesses follow the trend of the laboratory data (equation (2*a*)) quite closely, but do not agree with the "time-average" equation (2*b*) or with the trend of the older downhole log data observed by *Carlson and Raskin* [1984], either because of the age of the crust at site 418, or because of the poor quality of the old downhole log data. These results suggest that the empirical density/slowness relation which applies to the laboratory data (equation (2*a*)) also applies to typical oceanic crust, and that the mean density of oceanic crust older than 30 to 40 Ma is close to 2.86 Mg m^{-3}. Whether the old log data are representative of very young oceanic basement was unresolved.

4. Analysis of Downhole Logs: Holes 395A and 418A

To refine the models and determine which, if either, of equations (2) applies to young oceanic crust, we have undertaken new analyses of downhole log data from holes 395A and 418A. Conditions at site 395 differ from those at 418 in two significant respects. Hole conditions at 395A are comparatively poor; large breakouts occur in several places, and small washouts are common [*Bryan et al.*, 1988]. In consequence, the logs must be evaluated and interpreted with care to avoid spurious results. The second important difference is that the smectites from site 395 do not contain potassium (C. Broglia, personal communication, 1988), and the method used by *Broglia and Moos* [1988] to correct neutron porosities for smectite content cannot be applied to the hole 395A neutron porosity data. All of the several ways of calibrating the logs by using measurements made on core samples are essentially arbitrary. We have taken an alternative approach as described below, and applied our corrections to both the 395A and 418A log data so that the results can be meaningfully compared. We have also edited and reprocessed the sonic logs from both holes.

The long-spaced sonic tool is a seismic (sonic) refraction device. Two transmitters and two receivers are configured so that refracted sonic-wave traveltimes are measured over distances of 8, 10 and 12 ft. The velocity of the formation is determined for 2 ft. intervals by taking the differences of the 8 - to - 10 and 10 - to - 12 ft. measurements. In the usual mode of operation six travel time measurements are made (two each over 8, 10, and 12 ft.) at 6-inch (0.1524-m) intervals. In total, eight time differences over the same 2-foot interval can be computed, though they are not entirely independent because they have just two measurements of travel time over 10 ft. in common. In "standard" calculations long-spaced and short-spaced sonic travel times are determined separately, and each is based on two traveltime differences. R. Jarrard (personal communication 1988) has used combinations of four and eight differences. After some experimentation, we decided to use all eight traveltime combinations, treating them as independent estimates. In the process, we also edited the raw traveltime data. To remove some of the effects of noise and cycle skipping, we deleted time differences corresponding to velocities less than 2 or more than 7 km s^{-1}. In the case of hole 418A more than 95% of the data survived the editing process. Less than 82% were within acceptable limits in the case of 395A. This difference reflects the difference in borehole conditions in at the two sites. We used the remaining differences to calculate the mean slowness and the 95% confidence limit for each 2 ft. interval.

Aside from comparing logged gamma-gamma densities with the densities of core samples from massive flow units, little can be done to correct the density logs. *Carlson et al.* [1988] did recognize one editing measure that can be taken. Because raw neutron porosities overestimate in situ values, densities calculated from the neutron porosities and reasonable grain and pore fluid densities (2.93 Mg m^{-3}, 1.025 Mg m^{-3}) represent the minimum possible in situ densities; corresponding gamma-gamma densities which fall below this limit must be spurious. We have used this criterion to edit the density logs from holes 395A and 418A.

Correcting the neutron porosity logs is a more difficult problem. As noted by *Broglia and Moss* [1988] these logs can be calibrated only by comparison with the properties of the recovered cores. We have assumed that the core samples from holes 395A and 418A are sufficiently representative of the range of in situ compositions (grain densities) to establish statistically valid trends relating in situ porosities to in situ densities. We began by averaging the log values over 50-point intervals and crossplotting the averaged log values and the core data [*Melson et al.*, 1979; *Donnelly et al.*, 1980] as shown in Figure 4.

Standard linear regression assumes that the independent variable is error-free, but there are uncertainties in both the densities and porosities from the downhole logs (Figure 4). The coefficient values obtained by linear regression then depend on which variable is taken to be independent. Of several methods that can be used to overcome this problem, we have chosen to use functional analysis [e.g., *Davies and Goldsmith*, 1972; *Mark and Church*, 1977], which takes into account the errors in both variables and yields a single set of coefficients. In the case of the hole 418A core data, the five data points having the lowest densities and the highest porosities were not used in the statistical

TABLE 1. Summary of Structural Analysis Parameters

	b_0	b_1	N	r^2	SE $Mg\text{-}m^{-3}$
		418A			
Raw lab data	3.01 ± 0.01	-3.41 ± 0.12	93	0.88	0.035
Corrected	3.01 ± 0.01	-3.10 ± 0.12	-	-	-
Raw log data	3.05 ± 0.03	-1.73 ± 0.14	30	0.83	0.036
		395A			
Lab data	2.97 ± 0.02	-2.14 ± 0.09	81	0.86	0.024
Raw log data	3.04 ± 0.06	-1.55 ± 0.11	53	0.74	0.066

analysis. The results of these analyses are summarized in Table 1.

In both cases, the distribution of the log data is linear (Figure 4, Table 1), the standard errors are reasonably small, and the coefficients of determination are high, suggesting that the internal consistency and precision of the density and porosity logs are qualitively good. However, the trends of these data (Figure 4, Table 1) require a significant, systematic increase in grain density with increasing fractional porosity. Such a relationship is not physically reasonable. The raw neutron porosities are clearly too high and the degree to which they overestimate true in situ porosities increases with decreasing bulk density. This phenomenon is perhaps to be expected. In the 418A section, low densities reflect both higher degrees of alteration and higher porosities [e.g., Figure 4 of *Broglia and Moos*, 1988]. It is also widely recognized that alteration is related to permeability, which is at least loosely related to porosity. Thus, parts of the logged interval having higher porosities and higher (implied) initial permeabilities may be expected to have higher volume fractions of alteration products and hence of bound water; the extent to which neutron porosites overestimate in situ porosities must then increase with increasing porosity or decreasing density.

The trends shown by the densities and porosities of the core samples (Figure 4) are also interesting. In each case there is an apparent, systematic decrease of grain density with increasing porosity, though it should be noted that this tendency is not statistically significant in the 395A core data (Table 1). In contrast, the apparent change is both significant and dramatic in the 418A data. *Broglia and Moos* [1988] attributed this trend to systematic errors in the measured porosities. Indeed, *Donnelly et al.* [1980] assert that the core porosities measured in the shipboard laboratory might be low by as much as 10 percent. In an independent study of core samples from sites 417 and 418, *Christensen et al.* [1980] observed a similar trend, but to account for the apparent decrease in grain densities with decreasing bulk densities, the measured porosities would have to be in error by a factor of nearly 2. Errors of this magnitude are hard to accept and we believe there is an alternative explanation. Here our line of argument closely parallels the explanation we have proposed above for the trends in the uncorrected log data. Alteration products such as smectites have significantly lower densities than do the primary mineral phases found in fresh basalts. Mean grain densities must therefore decrease with increasing alteration, and if the degree of alteration increases with increasing porosity, we must expect a systematic relationship between grain density and porosity. The rate of change of grain density with porosity is likely to be non-linear (i.e., a function of porosity), but if we may approximate it by a constant (at least for a limited range of porosities) bulk density becomes a quadratic function of porosity

$$\rho_b = \rho_{go} + [\rho_f - \rho_{go} - (\partial\rho_g/\partial\Phi_f)]\,\Phi_f + (\partial\rho_g/\partial\Phi_f)\Phi_f^2 \quad (3)$$

where ρ_b is bulk density, ρ_{go} is the density of the unaltered solid, ρ_f is the pore fluid density, Φ_f is fractional porosity.

For the 418A core data, this relationship is approximately

$$\rho_b = 3.0 - 3.2\Phi_f + 1.2\Phi_f^2 \quad (4)$$

The core data do suggest a relationship of this general form (Figure 4). Unfortunately, the data are not sufficient to explore this interesting phenomenon further.

Having convinced ourselves that the core data are not seriously affected by systematic errors and that the range of compositions (grain densities) represented by the core samples is sufficient to establish well-constrained statistical relationships (Table 1), we have assumed that the log data should conform to the trend of the core data. We corrected the neutron porosities accordingly, by estimating the necessary correction equations from the functional analysis coefficients (Table 1). In the case of hole 418A, we have adjusted the correction for a 10% error in the porosities of the core samples:

$$418A \qquad \Phi_c = 0.56\,\Phi_a - 0.01;\ \varepsilon = 0.055 \quad (5a)$$

$$395A \qquad \Phi_c = 0.72\,\Phi_a - 0.03;\ \varepsilon = 0.030 \quad (5b)$$

where Φ_c is the corrected neutron porosity, Φ_a is the apparent porosity, and ε is the error (or precision) arising from the correction.

After correcting the 395A and 418A downhole logs, we averaged the logged values over 7.75-m intervals (52 points) and computed the 95 percent confidence intervals of the estimated means. We computed averages over the same intervals from the 418A neutron porosity and sonic logs as processed by *Broglia and Moos* [1988] for comparison. The results are summarized in the appendix[1](Tables A1-A3).

Crossplots of the corrected densities and porosities are also shown in Figure 4. Of particular interest are the plots of density versus smectite-corrected porosity [*Broglia and Moos*, 1988] and "trend-corrected" porosity (this study). On average the smectite-corrected fractional porosites are about 0.05 (5 p.u.) higher than

1 The appendix is available with the entire article on microfiche. Order from American Geophysical Union, 2000 Florida Avenue, N.W., Washington, DC 20009. Document B90-001; $2.50. Payment must accompany order.

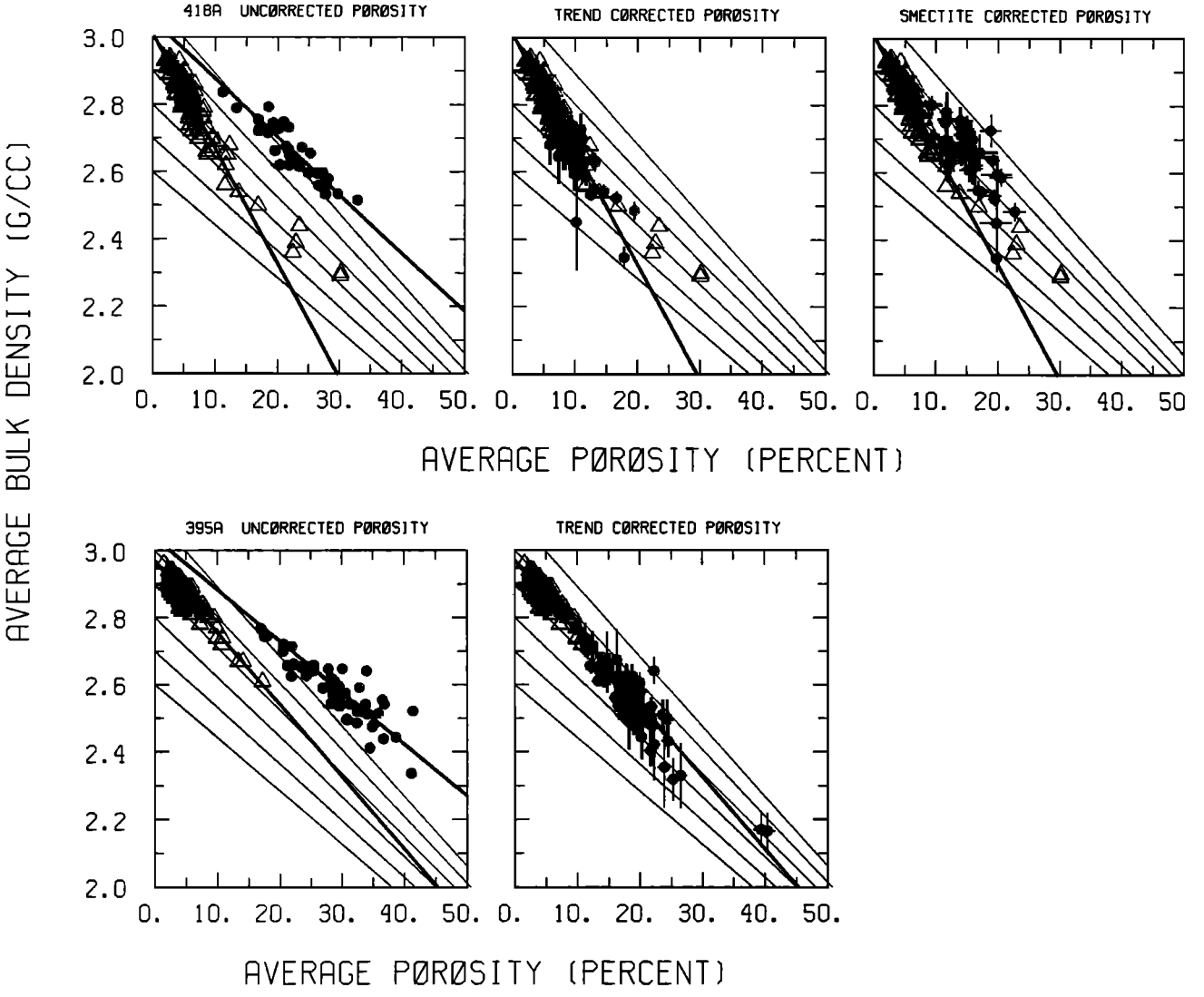

Fig. 4. Density versus porosity in core samples (triangles) and raw and corrected logs (dots) from holes 418A and 395A. Light diagonal lines are lines of constant grain density; 2.6 through 3.1 Mg m-3 at intervals of 0.1 Mg m-3, as indicated by their intercept values. Heavy lines show fits to the data by functional analysis. Error bars associated with log values indicate 95 percent confidence limits of average of 52 log data points (7.8m). Hole 418A, top: left, core data and uncorrected log data; center porosities corrected to trend of core data (this study); right, porosities corrected for smectite (bound water) content [*Broglia and Moos*, 1988]. Hole 395A bottom: left, core and uncorrected log data; right, porosities corrected to trend of core data.

ours. We cannot argue that either correction is more appropriate than the other because both correction schemes are essentially arbitrary. However, we do note that the smectite correction increases the scatter in the data to some degree. The increased scatter probably arises from the fact that some of the potassium in hole 418A occurs in potassium feldspars as opposed to smectities, particularly in the upper part of the section [*Humphris et al.*, 1980].

The two sets of hole 418A logs are plotted versus depth in Figure 5. Open boxes represent the logs processed by *Broglia and Moos* [1988]. Solid boxes represent the results from this study. The width of each box indicates the 95% confidence interval of the mean for the depth interval shown by the height of the box. Densities are common to both sets of logs and are therefore the same. It should be noted that the estimated errors for the two sets of velocity and porosity data are not directly comparable. In the data provided by *Broglia and Moos* [1988], we have only the populations of values themselves from which to estimate errors. In our own reduction of the sonic and neutron porosity logs, we estimated the uncertainties in the corrected log values. Our estimated errors in the mean values are smaller only because we have more information regarding the statistical properties of the data. In general the mean velocities agree well. The porosities estimated in this study are lower by about 0.05, as noted previously.

Several features of these logs (Figure 5) are worthy of note. Strong vertical gradients are indicated above about 250 msb. The density data are not sufficient to estimate the gradient, but weighted least squares fits indicate that the porosity and velocity gradients are -0.08 ±0.01 p.u. m^{-1} (porosity units) and 7 ±1 s^{-1}, respectively. The latter is comparable with velocity gradients detected by seismic refraction methods in the uppermost oceanic crust [e.g., *Purdy*, 1983; *Vera and Mutter*, 1988]. Below 250 msb, porosities range from 0.05 to about 0.13, and velocities ranging from about 5.0 to 5.7 km s^{-1} are typical of layer 2b (5.2± 0.4km s^{-1}). Near the top of the logged interval, average velocities range from 4 to 4.5 km s^{-1}. Though it has been asserted that layer 2a is absent at this site [e.g. *Salisbury et al.*, 1986; *Moos*, 1988;

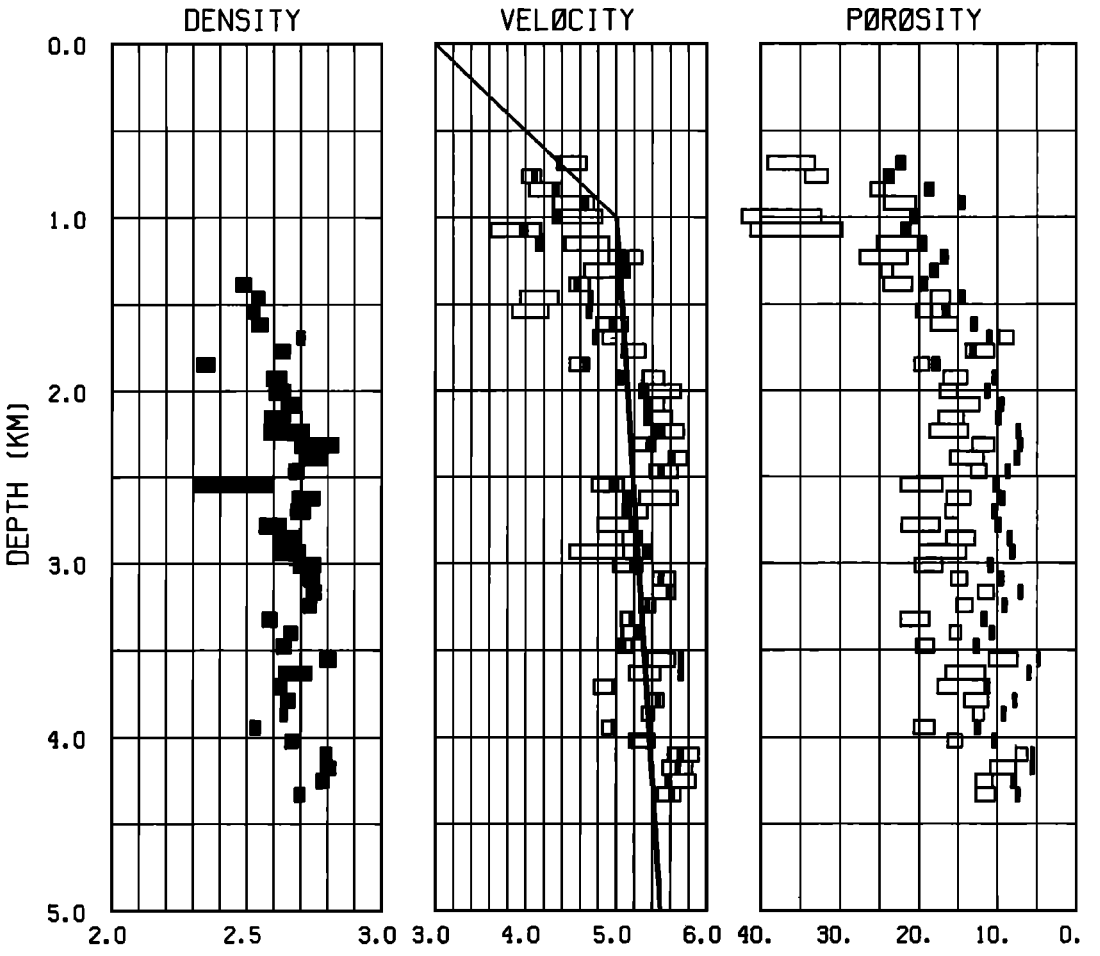

Fig. 5. Average log data from hole 418A. The width of each box represents the 95% confidence interval of the mean calculated for the depth interval represented by the height of each box (about 7.8 m). Open boxes, data from *Broglia and Moos* [1988]. Solid boxes, this study. Note strong gradients above 250 msb. Note also the excellent agreement between the velocities observed at 418A and the average velocity structure of 140 Ma-old crust [*Purdy*, 1983], indicated by the heavy line.

Salisbury et al., 1988a], these velocities are in fact transitional between those typical of layer 2a and 2b (3.7 ± 0.4 and 5.2 ± 0.4 km s^{-1}). *Swift et al.* [1988] also reported transitional velocities (about 4.5 km s^{-1}) near the top of the basement section in the vicinity of hole 418A, based on the results of their oblique seismic experiment. *Purdy* [1983] inferred the existence of a region of similarly low velocities in old western North Atlantic crust and the hole 418A sonic log data are quite consistent with *Purdy's* [1983] average velocity structure model (heavy line, Figure 5).

While it would be dangerous to assume that the sections penetrated by holes 395A and 418A may be taken as typical of young and old oceanic crust, it is nevertheless interesting to compare the logs. The average logs (this study) are illustrated in Figure 6. In these data sets, the uncertainties have been calculated in the same way. Densities at site 395A are about 0.2 Mg m^{-3} lower than those at 418A, and do not show a similar strong gradient near the top of the hole. Instead, the densities increase gradually from 2.4 to 2.5 Mg m^{-3} to 2.6 to 2.7 Mg m^{-3} over the logged interval. Similarly, the corrected porosities from 395A decrease gradually, from 0.20 to 0.25 near the top of the section to 0.10 to 0.15 at the bottom, and are appreciably higher than those at 418A. On average, the difference is 0.07 (7 p.u.). The sonic log from hole 395A is badly affected by hole conditions. We deem these data to be unreliable over large intervals of the logged section as indicated by the absence of corresponding averaged values in Figure 6. Breakouts are likely to occur where cracks are prevalent and low velocities may be expected. We therefore suspect that the reliable velocities are biased toward higher values. These velocities are generally in the range 4.8 to 5.6 km s^{-1} and are typical of layer 2b. The high velocities near the top of the section represent massive flows. Elsewhere, velocities at 395A tend to be 0.2 to 0.4 km s^{-1} lower than those at 418A. Though conditions at sites 395 and 418 may not be representative of young and old oceanic crust, it can be said that the observed differences in in situ physical properties are consistent with prevailing ideas regarding alteration and aging of the uppermost crystalline basement.

5. Density, Porosity, and Velocity Systematics

To this point we have focused on the downhole logs from holes 395A and 495A, and on the properties of the uppermost oceanic basement sections at those sites. We now seek to generalize the results so that they can be applied to the oceanic crust and to test the empirical density/velocity relationships proposed by *Carlson and Raskin* [1984]. To that end we have made weighted least squares fits of the averaged densities and porosities on the averaged slownesses from the downhole log data (Tables A1-A3). In making the fits we have neglected the errors in mean slowness on the grounds that they are small and comparatively uniform, so the results should not be seriously affected by this procedure. The

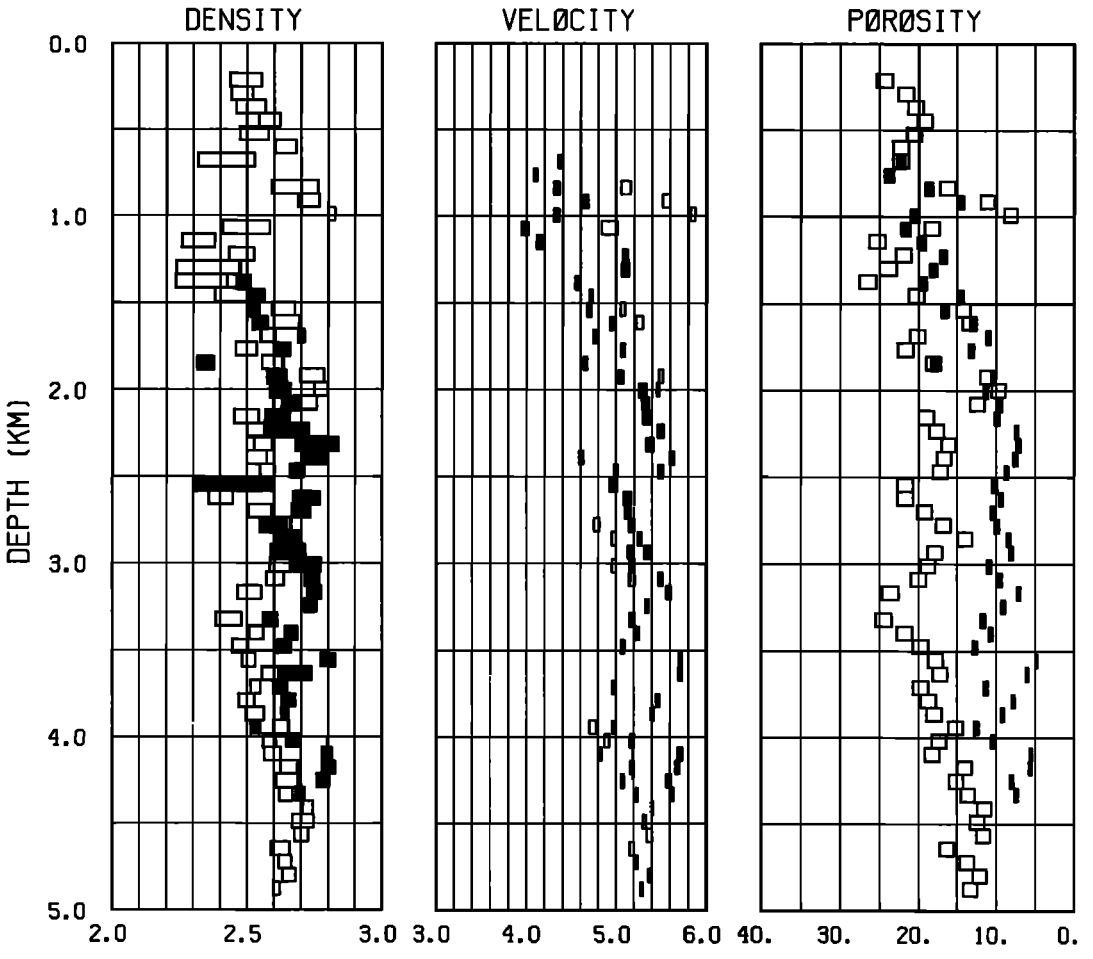

Fig. 6. Average log data from holes 395A (open boxes) and 418A (solid boxes). Symbols otherwise as in Figure 5.

results are summarized in Figure 7 and Table 2. The relationships proposed by *Carlson and Raskin* [1984] are included in Table 2 for comparison.

At this point, we must stress that the estimated errors in the corrected data (Tables A1-A3), and hence the errors in coefficients estimated from the fits (Table 2), represent precision, not accuracy. We have no way of assessing systematic errors. We believe the accuracies of the density and sonic log data to be good, but the corrected neutron porosities may be subject to systematic error, as evidenced by the difference between our results and those of *Broglia and Moos* [1988].

The fits of density on slowness are characterized by comparatively small standard errors (<0.1 Mg m^{-3}), but the coefficients of determination are also low and the errors in the coefficients are quite large owing to the narrow range of the data relative to scatter. The fit to the hole 418A data produced coefficients having values intermediate between those of the time-average equation (2*b*), and the fit to the laboratory data (2*a*); it is

TABLE 2. Weighted Linear Regression Parameters: Density and Porosity vs. Slowness

	b_o	b_1 s,km^{-1}	N	r^2	SE $Mg\text{-}m^3$
Density Mg m^{-3}					
Time-average [a]	3.50 ± 0.2	-3.79 ± 0.1	-	-	-
Laboratory data [a]	3.81 ± 0.02	-5.99 ± 0.11	483	0.86	0.07
418A	3.61 ± 0.16	-4.95 ± 0.81	40	0.49	0.07
395A	3.78 ± 0.14	-5.86 ± 0.73	30	0.70	0.04
Combined [b]	3.66 ± 0.11	-5.24 ± 0.57	70	0.56	0.06
Fractional Porosity					
418A	-0.35 ± 0.03	2.37 ± 0.15	49	0.84	0.015
395A	-0.27 ± 0.07	2.16 ± 0.34	30	0.58	0.02
Combined [b]	-0.36 ± 0.03	2.42 ± 0.14	79	0.79	0.017

[a] from *Carlson and Raskin [1984]*
[b] "combined" denotes data from 395A and 418A.

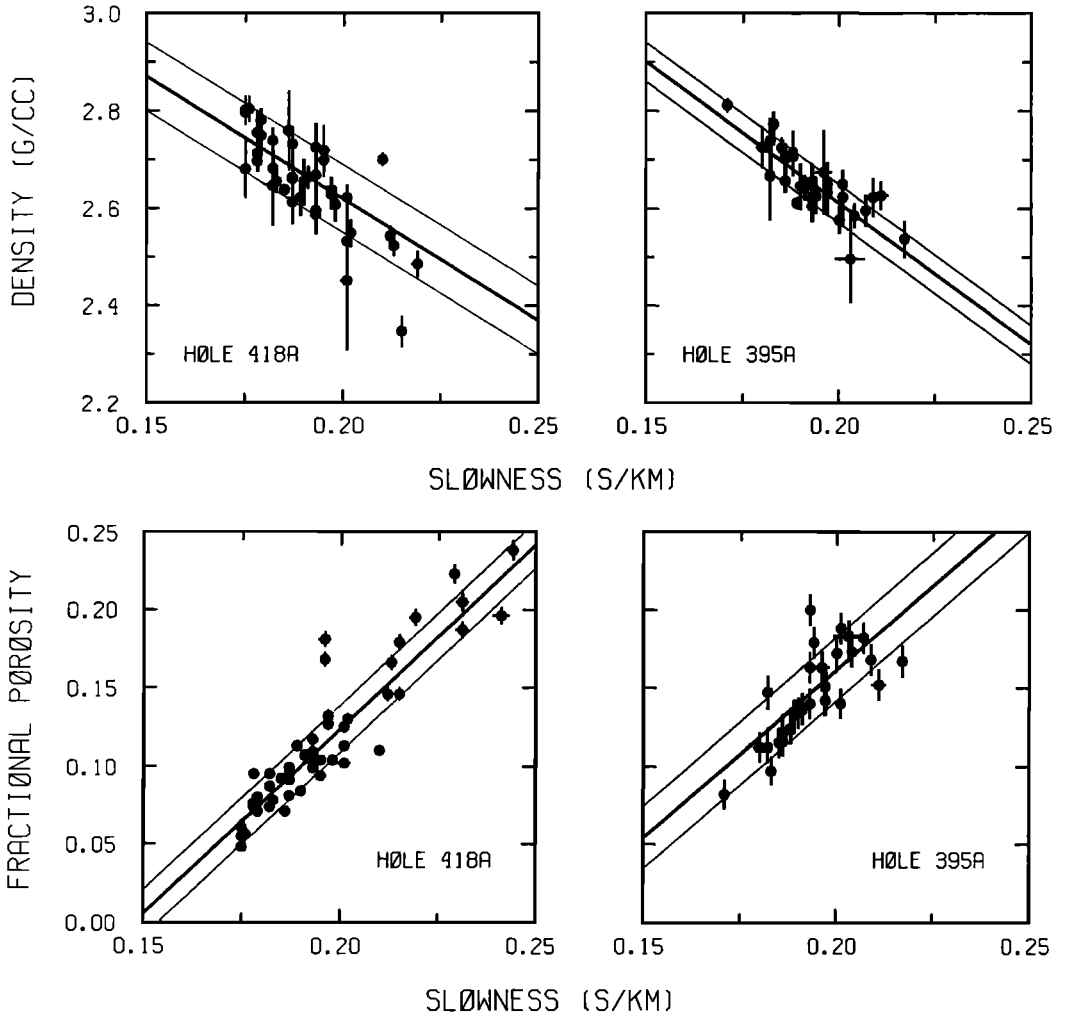

Fig. 7. Weighted least squares fits of in situ density and porosity on slowness from holes 418A and 395A. Error bars indicate 95% confidence limits of mean densities and porosities. Solid lines indicate best fits to the data; light lines indicate standard error.

in slightly better agreement with the latter, but is not distinguishable from either at the 95 percent confidence level. Fits to the averaged log values from hole 395A and to the combined data (Table 2) both differ significantly from the time-average equation (2b), but are undistinguishable from the fit to the laboratory data (equation 2*a*). The fit to the 395A log data is virtually identical to that for the laboratory data, but we must emphasize that the data set has been heavily edited owing to the effect of breakouts on the sonic log, and the 395A data set, taken by itself, should not be taken as representative of the logged interval, much less of young oceanic crust. Though these results are not as conclusive as we might have liked , they do indicate that the in situ density/velocity relation does not differ significantly from equation (2*a*). We therefore conclude that (2*a*) is the best available empirical equation relating in situ densities to seismic velocities for both young and old oceanic crust. The trend of the old downhole log data [*Carlson and Raskin* 1984] is spurious, and probably reflects systematic errors in the raw data from which averages were computed.

Fits of porosity on slowness are also summarized in Table 2 and Figure 7. The errors in the coefficients (Table 2) are large, again owing to the small range of the data, and the three fits are not statistically different. The standard errors are comparitively small, about 0.02 (2 p.u.). The fit to the data from hole 418A has a particularly high coefficient of determination, suggesting that the neutron porosity data from hole 418A are significantly less noisy than the densities. To estimate porosities from seismic velocities we have used the fit to the 418A data

$$\Phi_f = (-0.35 \pm 0.03) + (2.37 \pm 0.15)S \quad (6)$$

though we again stress the point that the results may be subject to systematic error.

6. Density and Porosity Structure of the Oceanic Crust

We used the empirical density/velocity and porosity/velocity relationships (equations (2*a*) and (2*b*)) to estimate in situ densities and porosities from average crustal velocity-structure models. The results are presented in Table 3. We based our estimates on the same eight structure models used by *Carlson and Raskin* [1984], but with some refinements. Where they used population variances to estimate errors in the calculated densities and porosities and did not include errors in layer thickness in some cases, we have estimated errors in the mean velocities and mean thicknesses (Table 3). Where the numbers are available, the errors were estimated from the original published compilations [*Raitt*, 1963; *Christensen and Salisbury*, 1975; *Houtz and Ewing*, 1976]. When errors in velocity could not be computed, we have taken the error

TABLE 3. Summary of Average Crustal Properties

Source	Layer	Thickness km	Velocity km s^{-1}	Density mgm^{-3}	Fractional Porosity
Raitt [1963]	2	1.71 ± 0.10	5.07 ± 0.08	2.629 ± 0.035	0.117 ± 0.042
	3	4.86 ± 0.17	6.69 ± 0.02	2.915 ± 0.026	0.004 ± 0.036
Means				2.840 ± 0.022	0.034 ± 0.029
Shor et al. [1971]	2	1.49 ± 0.10	5.19 ± 0.09	2.656 ± 0.035	0.107 ± 0.042
(Pacific Basin)	3	4.62 ± 0.17	6.81 ± 0.03	2.930 ± 0.026	0.000 ± 0.000
Means				2.863 ± 0.022	0.026 ± 0.010
Christensen and Salisbury [1975]	2	1.39 ± 0.06	5.04 ± 0.09	2.622 ± 0.036	0.120 ± 0.042
(age greater than 40 Ma)	3	4.97 ± 0.17	6.73 ± 0.03	2.920 ± 0.026	0.002 ± 0.036
Means				2.855 ± 0.022	0.028 ± 0.030
Christensen and Salisbury ([975]	2	1.60 ± 0.10	4.40 ± 0.10	2.449 ± 0.045	0.189 ± 0.04
(sonobuoy type I)	3a	1.20 ± 0.06	6.40 ± 0.03	2.874 ± 0.027	0.020 ± 0.037
	3b	4.40 ± 0.20	7.10 ± 0.03	2.966 ± 0.026	0.000 ± 0.000
Means				2.836 ± 0.020	0.045 ± 0.012
Christensen and Salisbury [1975]	2	1.60 ± 0.10	4.40 ± 0.10	2.449 ± 0.045	0.189 ± 0.047
(sonobuoy type II)	3a	3.00 ± 0.15	6.80 ± 0.03	2.929 ± 0.026	0.000 ± 0.000
	3b	2.60 ± 0.13	7.50 ± 0.03	3.011 ± 0.025	0.000 ± 0.000
Means				2.852 ± 0.018	0.042 ± 0.011
Houtz and Ewing [1976]	2a	0.30 ± 0.02	3.74 ± 0.10	2.208 ± 0.056	0.284 ± 0.053
(Atlantic)	2b	0.97 ± 0.04	5.13 ± 0.04	2.642 ± 0.031	0.112 ± 0.041
	2c	0.91 ± 0.09	6.05 ± 0.03	2.820 ± 0.027	0.042 ± 0.038
	3	4.97 ± 0.17	6.83 ± 0.03	2.933 ± 0.026	0.000 ± 0.000
Means				2.849 ± 0.019	0.032 ± 0.008
	2a	0.44 ± 0.02	3.47 ± 0.09	2.084 ± 0.058	0.333 ± 0.05
Houtz and Ewing [1976]	2b	0.80 ± 0.04	5.28 ± 0.04	2.676 ± 0.030	0.099 ± 0.041
(Pacific)	2c	0.93 ± 0.12	6.12 ± 0.03	2.831 ± 0.027	0.037 ± 0.038
	3	4.97 ± 0.17	6.90 ± 0.03	2.942 ± 0.026	0.000 ± 0.000
Means				2.845 ± 0.019	0.036 ± 0.008
Purdy [1983]	2a	0.10 ± 0.02	4.05 ± 0.10	2.331 ± 0.050	0.235 ± 0.049
(Atlantic, 140 Ma)	2b	0.50 ± 0.02	5.35 ± 0.10	2.690 ± 0.036	0.093 ± 0.041
	2c	1.80 ± 0.04	6.13 ± 0.04	2.833 ± 0.028	0.037 ± 0.038
	3a	1.60 ± 0.09	6.83 ± 0.03	2.933 ± 0.026	0.000 ± 0.000
	3b	3.10 ± 0.16	7.00 ± 0.03	2.954 ± 0.026	0.000 ± 0.000
Means				2.891 ± 0.015	0.019 ± 0.010

in average "layer 2" velocity to be about 0.1 km/sec and the error in mean "layer 3" velocity to be 0.03 km s^{-1}. Similarly, where layer thicknesses could not be estimated from the published data, we have taken the error to be 5%. We have also assumed in situ porosities in layers having velocities greater than about 6.8 km s^{-1} to be negligible.

The density structures determined from the various structure models (Table 3) are quite consistent. In general, layer 2 densities (including averages for layers 2a, 2b and 2c) range from 2.62 to 2.69 Mg m^{-3}. Average layer 2a densities are less than about 2.3 Mg m^{-3}, average layer 2b densities range from 2.64 to 2.69 Mg m^{-3}, and the average density of layer 2c is 2.83 ± 0.03 Mg m^{-3}. The average density of layer 3 (including layers 3a and 3b) is in the range 2.92 to 2.97 Mg m^{-3}. Average crustal densities range from 2.84 to 2.89 Mg m^{-3}, with a grand average of 2.86 ± 0.03 Mg m^{-3}.

The estimated porosities are also quite consistent. In general, estimated layer 2 porosities (again including the averages for layers 2a, 2b, and 2c) are in the range 0.10 to 0.12 (10 to 12 p.u.). An exception is that *Purdy's*[1983] model for old oceanic crust yields an average layer 2 porosity of 0.06. Layer 2a porosities are in the range 0.24 to 0.33, while the estimated porosities for layer 2b are about 0.10. Estimated layer 2c porosities (0.04 ± 0.04) are uniform, but not statistically significant. The estimated average porosities for the crust are also not statistically significant (Table 3), but we may conclude that the porosity of the crust as a whole is less that about 5 %.

Most of the average crustal structure models cannot be meaningfully compared with the downhole logging results, but *Purdy's* , [1983] model applies to 140 Ma-old crust in the western North Atlantic, and hole 418A penetrated crust of roughly comparable age [110 Ma] in the same region. We have previously noted that Purdy's velocity structure model for the uppermost oceanic crust compares favorably with the sonic velocities from hole 418A (Figure 6). Porosities in the upper part of the logged interval (Figure 6) are in the range 0.20 to 0.25, and are thus consistent with the porosity of layer 2a (0.24 ± 0.05) estimated from Purdy's model (Table 3). Log densities are not available for the upper part of hole 418A, but if they follow the trend of the porosities, they would fall in the range 2.3 to 2.5 Mg m^{-3} and would be comparable with the calculated density of layer 2a (2.3 ± 0.04 Mg m^{-3}). Similarly, below 250 msb in hole 418A, the sonic velocities are characteristic of layer 2b, and the densities and porosities average about 2.7 Mg m^{-3} and 0.10 (10 p.u.), respectively. The density and porosity of layer 2b estimated from *Purdy's* [1983] model for 140-Ma-old crust are 2.69 ± 0.04 Mg m^{-3} and 0.09 ± 0.04 (Table 3). Thus the densities and porosities

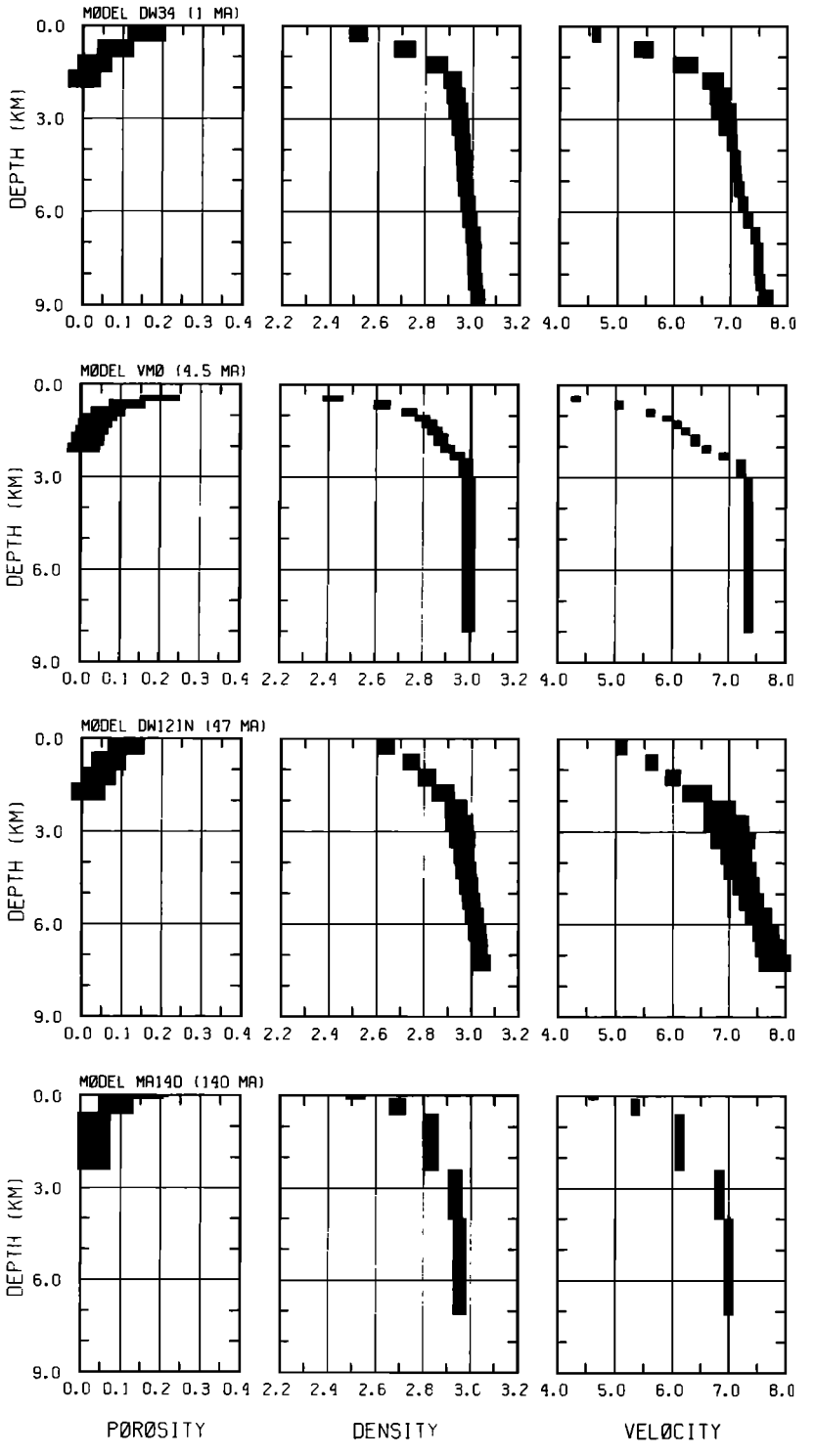

Fig. 8. Selected velocity, density and porosity profiles. Densities and porosities estimated from seismic velocity profiles: MA140 [*Purdy*, 1983], DW121N [*Kennett and Orcutt* 1976] DW34 [*Kennett and Orcutt*, 1976],VMO [*Vera and Mutter*, 1988]. Height of each box represents depth interval, width represents standard deviation.

estimated from seismic velocities are consistent with densities and porosities estimated from downhole logs.

The average structure models described above are useful, but fail to reveal details. For that purpose we have calculated densities and porosities from four published velocity profiles: *Purdy's* [1983] model for 140-Ma-old Atlantic crust, profiles DW34 (47 Ma) and DW12IN (1 Ma) form the ROSE area [*Kennett and Orcutt*, 1976] and an average model for 4.5-Ma-old crust, also on the East Pacific Rise [*Vera and Mutter*, 1988]. The model profiles are presented in Figure 8. The height of each box represents the interval over which the properties were calculated. Widths represent standard deviations. Errors in velocity were taken directly from the inversions of DW34 and DW12IN [*Kennett and Orcutt*, 1976]. For the other two models we have assumed the errors to be 0.1 km s^{-1}.

The properties of the upper 500 m of the crustal section are quite variable, but between 500 and 1000 msb, porosities are

typically in the range 0.05 to 0.15, and decrease rapidly to negligible values at a depth of about 2 km.

Densities increase rapidly from 2.5 Mg m^{-3} near the top of basement to 2.9 to 3 Mg m^{-3} at depths near 3 km, and density gradients in the lower crust (layer 3) are low.

Strong velocity, density and porosity gradients are thus characteristic of the upper part of the oceanic crust. In situ porosities, densities and velocities can be empirically related with comparatively high precision, and it is tempting to ascribe the increases of density and velocity with depth to the corresponding reduction in porosity. However, statistical correlations alone do not imply casuality. This point is emphatically demonstrated by the fact that velocities can increase if and only if the effective elastic modulus of the medium increases faster than its density; velocities must increase in spite of, and not because of the strong positive correlation between density and velocity.

Strong porosity gradients probably arise in several ways. (1) Some of the variation is doubtless of primary origin; massive flows and dikes deeper in the section lack the large voids and interstices that are common in the overlaying pillow lavas. (2) Large voids and porous rubble zones in the extrusive pile are likely to collapse or be compacted by overburden stresses [e.g., *Hyndman and Drury*, 1976] which increase with depth. This effect should not be confused with elastic closure of cracks and pore spaces by effective stress. Overburden stresses in the upper 2 km of the crust are too low (less that about 60 MPa) to cause a significant reduction of porosity by this mechanism [e.g., *Carlson and Gangi*, 1985; *Brown and Scholz*, 1985]. (3) The displacement of pore waters by solid alteration products will reduce porosities throughout the section.

In situ densities clearly reflect in situ porosities because the densities of both fresh basalts and alteration products are appreciably higher than the density of the fluid pore medium. The exact relationship between porosity and density also depends on the age of the crust or the degree of alteration. Over the upper 2 km of the basement section, the density and porosity gradients are approximately, + 0.3 Mg m^{-3} km^{-1} and -0.07 km^{-1}(Table 3, Figure 8), respectively. The density gradient can also be estimated from the variations of grain density and porosity with depth

$$\frac{d\rho_b}{dz} = [\rho_f - \rho_g(z)]\frac{\partial \Phi}{\partial z} + [1-\Phi(z)]\frac{\partial \rho_g}{\partial z} \quad (7)$$

Take ρ_{g-1} and $\Phi(z) \sim 0.15$ to $0.07z$ (for z in km; see Figure 8). We find from the hole 418A shipboard laboratory data [*Donnelly et al.*, 1980] that $\rho_g(z) \sim 2.8 + (0.20 \pm 0.03)\, z$. Based on these estimates, the average density gradient over the upper 2 km of the crust is 0.14 + 0.18 ~ 0.32 Mg m^{-3} km^{-1}, in excellent agreement with the observed density gradients (Figure.8). While we cannot say that the model values are strictly correct, we may conclude that they are mutually consistent and that the density gradients can be "explained" by the observed variations of porosity and grain density with depth. This result further suggests that less than half of the increase in bulk density with depth may be attributed to decreasing porosity; slightly more than half of the density change arises from increasing grain density, which reflects (at least is part) a progressive decrease in the intensity of hydrothermal alteration downward through the section.

Other lines of evidence also suggest that our models of porosity structure are not unreasonable. Based on drilling results from DSDP leg 37 on the Mid-Atlantic Ridge, *Hyndman and Drury* [1976] suggested that the porosity in layer 2a may exceed 0.20. *Spudich and Orcutt* [1980] have suggested that porosities as high as about 0.25 are required to explain observed differences between seismic P and S wave velocities and the properties of basalts measured in the laboratory. Based on observed velocity gradients, and assuming spherical pores, *Whitmarsh* [1978] estimated an upper limit of 0.30 at the top of the crust, decreasing to a few percent at a depth of 2 km.

The rapid variations of porosity and density with depth in the upper oceanic crust can be explained by the primary variations of porosity, compaction and alteration. The causes of high velocity gradients are more complex. Three potentially significant contributors to the high velocity gradients can be cited. (1) Velocities in layer 2 are controlled in part by porosity gradients [e.g. *Christensen*, 1978; *Hyndman and Drury*, 1976; *Spudich and Orcutt*, 1980]. Velocities will increase as pore water is replaced by solids having significantly higher elastic moduli. Furthermore, layer 2 is thought to be populated largely by cracks (as opposed to pores), in which case the observed variations in porosity are more than adequate to explain observed velocity gradients [*Whitmarsh*, 1978; *Spudich and Orcutt*, 1980]. (2) Layer 2 velocity gradients are also thought to reflect the systematic increase of the metamorphic grade of alteration products with depth [*Christensen*, 1978; *Christensen and Salisbury*, 1975; *Spudich and Orcutt*, 1980] both in ophiolites and in the oceanic crust (hole 504B). Though the details are not well defined, laboratory studies do show that velocities tend to increase with metamorphic grade [*Christensen*, 1978], and we have previously noted the apparent correlations of seismic layers 2c and 3 with greenschist and amphibolite grade mineral assemblages. 3) A long-overlooked cause of high velocity gradients in layer 2 is the effect of pressure on cracked media [*Vera and Mutter*, 1988]. It is now widely recognized that stresses acting across cracks are supported by the asperites which populate the crack walls, and increasing stresses can cause significant increases in the effective elastic moduli of the medium [e.g. *Brown and Scholz*, 1985; *Carlson and Gangi*, 1985]. The effect is most dramatic at low effective pressures [*Carlson and Gangi*, 1985], and it is reasonable to suppose the high velocity gradients in layer 2 reflect the influence of increasing over-burden stresses acting on the formation. *Vera and Mutter* [1988] have proposed such a model, and concluded that overburden pressures alone are sufficient to account for observed layer 2 velocity variations.

Elastic-wave velocities in cracked or porous media are also sensitive to the pore fluid pressure in the medium. *Christensen* [1984] has pointed out that in young crust where voids are open to the water column, pore pressures should be hydrostatic, but that this condition may be perturbed: Where basement is sealed by a cap of impermeable sediments, pore pressures will exceed hydrostatic pressure. Pore pressures may also be elevated in areas of active deformation (e.g. at subductive zones) and may be either higher or lower than hydrostatic in areas of active hydrothermal circulation. *Christensen's* [1984] experimental work has shown that over the range of confining pressures appropriate to the upper 2 km of the oceanic crust, pore pressure variations can give rise to changes in the P wave velocities in basalts and diabases amounting to 5 to 10%. The influence of pore pressure on the properties of the formation may be still greater. Hence, vertical and lateral variations in pore pressure might cause considerable variations in the seismic properties of layer 2. Boreholes tend to restore hydrostatic conditions so that logging results apply only to the hydrostatic case. Holes 395A and 504B both penetrated active hydrothermal systems. Low pore pressures at these sites are evidenced by a vigorous flow of water into the boreholes. However, *Anderson and Zoback* [1982] have estimated that pore pressures are only about 8 MPa lower than hydrostatic at site 504. Such a small pressure difference should not significantly alter the formation properties [e.g., Figure 3 of *Christensen*, 1984]. Elsewhere, at sites which are not near active plate boundaries, drilling has not revealed evidence of anomalous pore pressures, either in basement or in the overlying sediment column. Deep sea sedimentation rates are apparently so low that hydrostatic equilibrium is achieved in spite of the low permeability of the pelagic and hemipelagic sediments which blanket the seafloor. There is, for example, no evidence of disequilibrium pore pressures

at sites 417 and 418 [*Donnelly et al.*, 1980; *Salisbury et al.*, 1986, 1988b]. For these reasons, we suggest that pore pressures are likely to be very near hydrostatic in most of layer 2, and that most of the observed velocity variations arise from other causes.

7. Age Dependence of Layer 2a Properties

Average crustal models reveal much about densities and porosities in the oceanic crust, their average values and variations with depth, but contain little information regarding the age dependence of the properties of layer 2a. Drilling and downhole logging data are suggestive (Figure 7), but details are lacking because we have no data for ages greater than 10 or less than 110 Ma. To assess the properties of layer 2a, we have used the average velocities as given by *Houtz and Ewing* [1976] and the errors in the mean values to estimate mean slownesses, densities and porosities and their associated errors. We then made weighted, linear least-squares fits of thickness, velocity, slowness, density and porosity on age.

The results are summarized in Table 4 and Figure 9. The fits are well-constrained. The coefficients of determination are quite high (>0.7) and the standard errors are small (<10%), but several caveats which affect interpretations of these results must be cited. The data set is small and the errors in the data are comparatively large. Resolution is therefore low. For example, velocity and slowness are inversely related, yet their variations with age are described equally well by linear models (Figure 9, Table 4). Thus, though we would expect the age dependence of layer 2a properties to be non-linear (alteration rates should decrease as the hydrothermal system cools), the nonlinearity is not resolvable from these data. Also, the lowest observed velocities of layer 2a are outside the range of the downhole log data. In estimating densities and porosities from such low velocities we have, in effect, extrapolated the empirical porosity/velocity and density/velocity relationships beyond the range of the data we have used to constrain them. Systematic errors are more likely under these circumstances. Finally, we have neglected errors in age, which must be appreciable. For these reasons, the rates of change we obtained from the fits to the data must be regarded as approximate averages for the period 0 to 30 Ma.

Our fits of layer 2a thickness and velocity on age agree closely with those of *Houtz and Ewing* [1976], except that our coefficients of determination are appreciably higher (Table 4). We can offer no explanation for the difference, but based on the distribution of the data and the errors, we suggest that their coefficients are much too low. Layer 2a thins at an average rate in the range 20 to 45 m m.y.$^{-1}$, while the velocity within the layer increases by an average of 0.04 km s^{-1} m.y.$^{-1}$. The best-fitting rates of change of layer 2a density and porosity, and their 95 percent confidence limits, are 0.016 ±0.009 Mg m^{-3} m.y.$^{-1}$ and 0.005 ±0.003 m.y.$^{-1}$, respectively. Porosities and densities in holes 395A and 418A differ by about 0.07 and 0.2 Mg m^{-3}. If we assume that these differences reflect changes which occurred between 6 and 30 Ma at site 418, the average rates of change are 0.003 m.y.$^{-1}$ and 0.008 Mg m^{-3} m.y.$^{-1}$. Thus it can be argued that the rates of change estimated from the seismic properties of layer 2a [*Houtz and Ewing*, 1976] are statistically consistent with the rates of change inferred from downhole logs. More refined estimates will require additional seismic refraction and downhole logging data.

8. Summary and Conclusions

Based on drilling and downhole logging results from sites 395, 418 and 504, laboratory studies of oceanic rocks, and data from ophiolites, we have estimated densities and porosities in the oceanic crust by applying empirical density/velocity and porosity/velocity relations to various seismic crustal structure models. The results may be summarized as follows:

Assuming that the section penetrated in hole 504B is representative of the upper oceanic crust and that the ophiolite analogy is valid, the velocity structure of the oceanic crust is more sensitive to variations in alteration or metamorphic grade and porosity than to its primary igneous structure. In hole 504B, layer 2a is an interval of high porosities and permeabilities [*Becker et al.*, 1982; *Anderson et al.*, 1985] affected by low-temperature alteration [e.g., *Alt et al.*, 1986]. The top layer of 2b corresponds closely to changes alteration [*Alt et al.*, 1986] and porosity *Becker et al.*, 1982] and a marked reduction in permeability [*Anderson et al.*, 1985] within the extrusive pile. Velocities typical of layer 2c are sustained from the top of the dikes (within the basalt-to-dike transition zone) downward; the 2b/2c boundary thus correlates with the top of the dike complex, an abrupt decrease of porosity to values less than a few percent [*Becker et al.*, 1982] and the first appearance of greenschist facies alteration products. In ophiolites, the top of layer 3 occurs in the mid to lower levels of the sheeted dike section and corresponds to the transition from greenschist to amphiobolite grade alteration products [*Christensen*, 1978; *Salisbury and Christensen*, 1978; *Christensen and Smewing*, 1981]. These correlations suggest that layer 2c consists almost entirely of diabase dikes affected by greenschist facies alteration, while the top of layer 3 represents the first appearance of amphibolite grade alteration products, and that layer 3 includes the lower part of the sheeted dike section as well as the gabbros of the lower crust.

We have drawn several conclusions from our analyses of downhole logs from holes 395A and 418A. Crossplots of raw log

TABLE 4. Layer 2a Properties Versus Age (Ma)

	b_0	b_1 m.y.$^{-1}$	N	r^2	SE
Thickness, km					
Atlantic	1.66 ± 0.18	-0.034 ± 0.012	5	0.72	0.14 km
Pacific	0.77 ± 0.04	-0.020 ± 0.003	4	0.97	0.06 km
Velocity, km s^{-1}	3.25 ± 0.09	0.038 ± 0.01	8	0.72	0.16 km s^{-1}
Slowness, s km^{-1}	0.307 ± 0.007	-0.0027 ± 0.0006	8	0.78	0.012 s km^{-1}
Density, Mg m^{-3}	1.97 ± 0.05	0.016 ± 0.004	8	0.76	0.08 Mg m^{-3}
Fractional porosity	0.35 ± 0.02	-0.005 ± 0.001	8	0.75	0.03

Weighted linear regressions based on data from *Houtz and Ewing* [1976].

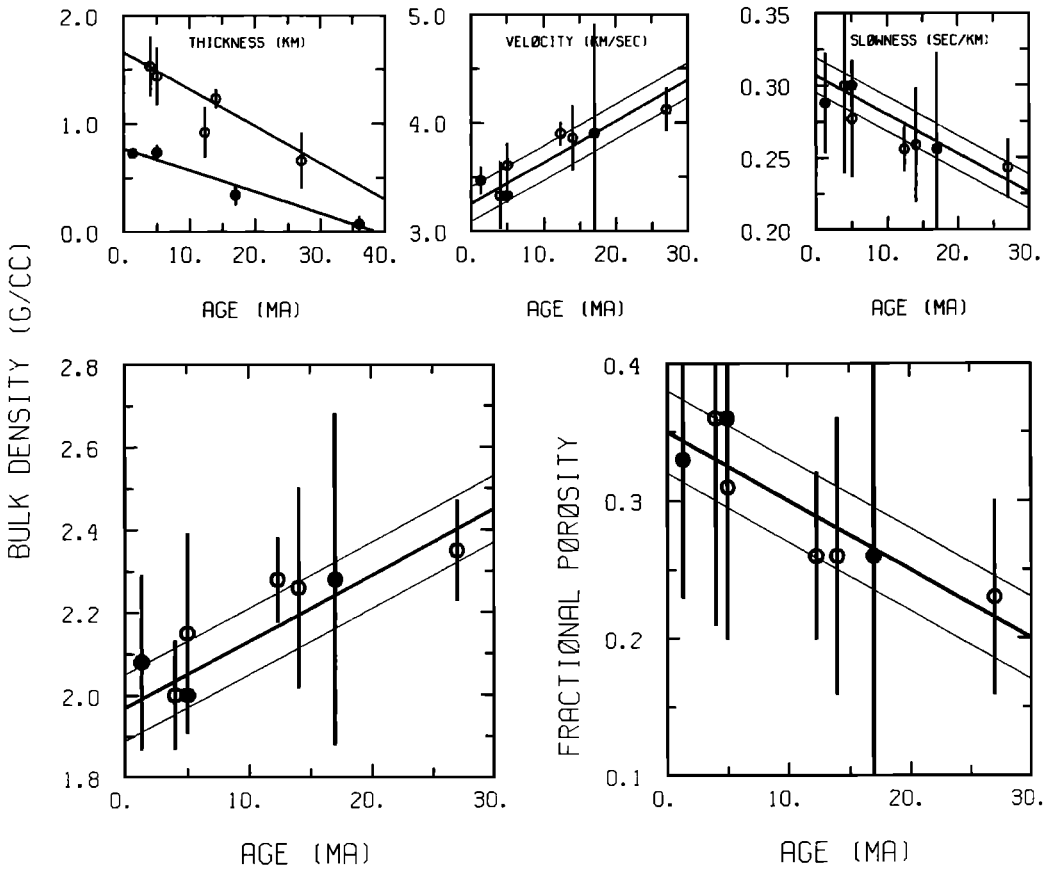

Fig. 9. Variations of layer 2a properties with age of seafloor. Velocity, thickness, and age data from *Houtz and Ewing* [1976]; open circles indicate data from the Pacific. Error bars indicate standard deviations of the means. Heavy line indicates weighted least-squares fit; light lines indicate standard error of estimate.

densities and porosities indicate an apparent increase in mean grain density with decreasing porosity, whereas the core data (from 418A in particular) show a trend of decreasing mean grain density with increasing porosity (Figure 4). We suggest that both trends may be explained if the degree of alteration increases with increasing porosity, as might be expected. Then increasing proportions of bound water will lead to systematically greater errors in neutron porosities, while larger volume fractions of low-density alteration products will give rise to a systematic decrease of mean grain density with increasing porosity in the cores.

The upper crustal sections drilled at sites 395 and 418 are not necessarily representative of young and old oceanic crust, though the sonic log velocities in hole 418A do compare very favorably with *Purdy's* [1983] seismic velocity structure model for 140-Ma-old Atlantic crust. Velocities near the top of hole 418A are transitional between the velocities of layers 2a and 2b, and velocities below 250 msb are characteristic of layer 2b. Porosities in hole 418A are about 0.07 (7 p.u.) lower than those in hole 395a, and bulk densities are about 0.2 Mg m^{-3} higher (Figure 3). These differences are consistent with prevailing views of the evolution of the uppermost oceanic crust.

To evaluate in situ physical properties systematics, we made weighted least squares fits of the log densities and porosities on slowness (Table 2, Figure 7). None of the fits of density on slowness is statistically distinguishable from the fit of laboratory densities on slowness by *Carlson and Raskin* [1984]; we take their fit to be the best available relationship between in situ density and seismic velocity. The "time average" relation proposed by Carlson and Raskin for oceanic layer 2 is apparently inappropriate for crust of any age. The relationship between in situ porosity and slowness is also highly linear, and we take the fit to the hole 418A log data to be the best relationship between in situ porosity and seismic velocity.

We used the empirical relationships to estimate in situ porosities and densities from eight average velocity structure models and four specific profiles representing a wide range of crustal ages (1 to 140 Ma; Table 3, Figure 8). The average models (Table 3) yield consistent results: the estimated bulk densities of layers 2a, 2b and 2c are, respectively, <2.3, 2.62 to 2.69 and about 2.83 Mg m^{-3}. The density of layer 2 is in the range 2.62 to 2.69 Mg m^{-3}, and the density of layer 3 ranges from 2.92 to 2.97 Mg m^{-3}. Estimated average crustal densities range from 2.84 to 2.89, with a grand average of 2.86 ± 0.03 Mg m^{-3}.

Estimated porosities may be subject to systematic errors arising from the corrections applied to the neutron porosity logs. The estimated fractional porosity of layer 2 is 0.10 to 0.12; the porosities of layers 2a, 2b and 2c are approximately 0.30, 0.10 and 0.04. In old Atlantic crust [*Purdy*, 1983] the estimated porosity of layer 2 is slightly lower, 0.06. Taking this number as a reasonable minimum, we estimate the weight fraction of water in the crustal section (not including bound water associated with hydrous mineral phases) to be on the order of 7 parts per thousand. If these pore waters survive the subduction process, the crystalline basement section alone is capable of delivering large quantities of water to the upper mantle.

Profiles of the crust (Figure 8) indicate that porosity and density gradients in the uppermost crust are high, approximately + 0.3 Mg m^{-3} km^{-1} and -0.07 km^{-1}, and mutually consistent. The density gradient reflects both a progressive reduction of porosity and an increase in grain density (which arises from the decreasing

intensity of alteration) with depth. Perhaps more significant for the purposes of this study is the fact that the porosities and densities estimated from the velocity structure of old Atlantic crust (*Purdy*, 1983) compare very well with the in situ values estimated from the hole 418A downhole logs. This fact indicates that in situ properties can be reasonably determined from seismic velocity structures.

Finally, we have estimated the rates of change of the properties of layer 2a based on the published data of *Houtz and Ewing* [1976]. From 0 to about 30 Ma, the velocity of layer 2a increases at an average rate of 0.04 km s^{-1} m.y.$^{-1}$ and the layer thins by 20 to 45 m m.y.$^{-1}$. The estimated average rates of change of layer 2 density and fractional porosity are 0.016 ± 0.009 Mg m^{-3} m.y.$^{-1}$ and 0.005 ± 0.003 m.y.$^{-1}$. These rates are statistically compatible with, but about a factor of 2 larger than, the rates we infer from the average in situ properties at sites 395 and 418. These numbers suggest that alteration leads to a net loss of pore water on the order of 5 kg m^{-3} m.y.$^{-1}$ and an associated total increase in solid mass (by exchange with seawater) on the order of 20 kg m^{-3} m.y.$^{-1}$.

Acknowledgements. We are particularly indebted to Cristina Broglia and Rich Jarrard of the Lamont-Doherty Geological Observatory for their invaluable assistance. Not only did they provide the logging data in usable form, they willingly lent us their expertise in numerous discussions. We are also grateful to the reviewers, Nik Christensen and Roy Wilkens. Their helpful suggestions significantly improved the paper. We would also like to thank Sandy Dunham and Crissy Richards, who prepared the camera-ready copy. The usual funding agencies declined to support this research, so we bootlegged it. We therefore gratefully acknowledge the Department of Geophysics and the Geodynamics Research Institute for bearing our computing and publication costs. Texas A&M Geodynamics Research Institute contribution 78.

REFERENCES

Alt, J.C., et al., Alteration of the upper oceanic crust, mineralogy and processes in Deep Sea Drilling Project hole 504B, leg 83, *Initial Rep. Deep Sea Drill. Proj., 83,* 217-247, 1985.

Alt, J.C., J. Honnerez, C. Laverne, and R. Emmerman, Hydrothermal alteration of a 1-km section through the upper oceanic crust, Deep Sea Drilling Project hole 504B: Mineralogy, chemistry, and evolution of seawater-basalt interactions, *J. Geophys. Res., 91,* 10,309-10,337, 1986.

Anderson, R. N., and M. D. Zoback, Permeability, underpressures, and convection in the oceanic crust near the Costa Rica Rift, equatorial Pacific, *J. Geophys. Res., 87,* 2860-2868, 1982.

Anderson, R.N., et al., DSDP hole 504B, the first reference section over 1 km through layer 2 of the oceanic crust, *Nature, 300,* 589-594, 1982.

Anderson, R.N. et al., *Initial Reports of the Deep Sea Drilling Project,* vol. *83,* U.S. Government Printing Office, Washington, D.C.,*1985a.*

Anderson, R.N., et al., Permeability versus depth in the upper oceanic crust: In situ measurements in Deep Sea Drilling Project hole 504B, eastern equatorial Pacific, *Initial Rep. Deep Sea Drill. Proj., 83,* 429-442, 1985b.

Becker, K., et al., In situ electrical resistivity and bulk porosity of the oceanic crust Costa Rica Rift, *Nature, 300,* 594-598, 1982.

Becker, K., et al., *Proceedings of ODP, Initial Reports,* vol. *111,* College Station, Texas, Ocean Drilling Program, 1988.

Broglia, C., and D. Moos, In-Situ structure and properties of 110-Ma crust from Geophysical logs in DSDP hole 418A, *Proc. Ocean Drill. Program, , Sci. Results, 102* , 29-47, 1988.

Brown, S.R., and C. H. Scholz, Closure of random elastic surfaces in contact, *J. Geophys. Res., 90,* 5531-5545, 1985.

Bryan, W.B., et al., *Proceedings of ODP, Initial Reports,* vol. *109,* Ocean Drilling Program, College Station, Tex., 1988.

Cann, J.R., and R.P. Von Herzon, Downhole logging at Deep Sea Drilling Project Sites 501, 504 and 505, *Initial Rep. Deep Sea Drill. Proj., 69,* 281-299, 1981.

Cann, J.R., et al., *Initial Reports of the Deep Sea Drilling Project,* vol. *69,* U.S. Government Printing Office, Washington D.C., 1983.

Carlson, R.L., and A.F. Gangi, The effect of cracks on the pressure dependence of *P* wave velocities in crystalline rocks, *J. Geophys. Res., 90,* , 8675-8684, 1985.

Carlson, R.L., and G.S. Raskin, Density of the ocean crust, *Nature, 311* , 555-558, 1984.

Carlson, R.L., K.R. Snow, and R.H. Wilkens, Density of old oceanic crust: An estimate derived from downhole logging on ODP leg 102, *Proc. Ocean Drill. Program, Sci. Results, 102,* 63-68, 1988.

Christensen, N.I., Ophiolites, seismic velocities and oceanic crustal structure, *Tectonophysics, 47,* 131-157, 1978.

Christensen, N.I., Pore pressure and oceanic crustal seismic structure, *Geophys.J. R. Astron . Soc., 79,* 411-423, 1984.

Christensen, N.I., and M.H. Salisbury, Structure and constitution of the lower oceanic crust, *Rev. Geophys., 13* , 57-86, 1975.

Christensen, N.I., and M.H. Salisbury, Seismic anisotropy in the oceanic upper mantle: Evidence from the Bay of Islands ophiolite complex, *J. Geophys. Res., 84,* 4601-4610, 1979.

Christensen, N.I., and M.H. Salisbury, Lateral heterogeneity in the seisimc structure of the ocean crust inferred from velocity studies of the Bay of Islands ophiolite, Newfoundland, Geophys. J. Roy. Astron. Soc., *68,* 675-688, 1982.

Christensen, N.I., and J.D. Smewing, Geology and seismic structure of the northern section of the Oman ophiolite, *J. Geophys. ,Res. 86,* 2545-2556, 1981.

Christensen, N.I., S.C. Blair, R.H. Wilkens, and M.H. Salisbury, Compressional Wave velocities, densities and porosities of basalts from Holes 417A, 417D and 418A, Deep Sea Drilling Project legs 51-53, *Initial Rep. Deep Sea Drill. Proj., 51-53,* 1467-1471, 1980.

CRUST, Geothermal regimes of the Costa Rica Rift, east Pacific , investigated by drilling, DSDP-IPOD legs 68, 69, and 70, *Geol. Soc. Am., Bull., 93,* 862-875, 1982.

Davies, O.L. and P.L. Goldsmith, *Statistical Methods in Research and Production,* 478 pp., Hafner, New York , 1972.

Donnelly, T., et al., *Initial Reports of the Deep Sea Drilling Project,* vol. *51-53,* U.S. Government Printing Office, Washington D.C., 1980.

Honnorez, J., et al., Stockwork-like sulfide mineralization in young oceanic crust: Deep Sea Drilling Project hole 504B, *Initial Rep. Deep Sea Drill. Proj., 83,* 263-282, 1985.

Houtz, R., and J.Ewing, Upper crustal structure as a function of plate age, *J. Geophys. Res., 81,* 2490-2498, 1976.

Humphris, S.E., et al., The mineralogy and geochemistry of basalt weathering, holes 417A and 418A, *Initial Rep. Deep Sea Drill. Proj., 51-53,* 1201-1218, 1980.

Hyndman, R.D., and M.J. Drury, The physical properties of oceanic basement rocks from deep drilling on the Mid-Atlantic Ridge, *J. Geophys. Res., 81,* 4042-4060, 1976.

Kennett, B.L.N., and J.A. Orcutt, A comparison of travel time inversions for marine refraction profiles , *J. Geophys. Res., 81,* 4061-4070, 1976.

Kirkpatrick, R.J., The physical state of the oceanic crust: results of downhole geophysical logging in the Mid-Atlantic Ridge at 23oN, *J. Geophys. Res., 84,* 178-188, 1979.

Lewis, B.T.R., Evolution of ocean crust seismic velocities, *Annu. Rev. Earth Planet., Sci., 6,* 377-404, 1978.

Little, S.A., and R.A., Stephen, Costa Rica Rift borehole seismic experiment, Deep Sea Drilling Project hole 504B, leg 92, *Initial Rep. Deep Sea Drill. Proj., 83,* 517-528, 1985.

Mark, D.M., and M. Church, On the misuse of regression in earth science, *Math. Geol., 9,* 63-75, 1977.

Melson, W.P., et al., *Initial Reports of the Deep Sea Drilling Project,* vol. *45,* U.S. Government Printing Office, Washington, D.C., 1979.

Molnar, P., and T. Atwater, Interac spreading and Cordilleran tectonics as alternates related to the age of subducted oceanic lithosphere, *Earth Planet. Sci. Lett.,* 41, 330-340, 1978.

Moos, D., Elastic properties of 110-Ma oceanic crust from sonic full-waveforms in DSDP hole 418A, *Proc. Ocean Drill. Program., Sci. Results, 102,* 49-62, 1988.

Morris, G.B., R.W. Raitt, and G.C. Shor, Jr., Velocity anisotropy and delay time maps of the mantle near Hawaii, *J. Geophys. Res., 74,* 4300-4316, 1969.

Newmark, R.L., et al., Sonic and ultrasonic logging of hole 504B and its implications for the structure, porosity and stress regime of the upper 1 km of the oceanic crust, *Initial Rep. Deep Sea Drill. Proj., 83,* 469-510, 1985.

O'Connell, R.J., and B. Budianski, Seismic velocities in dry and saturated cracked rocks, *J. Geophys. Res., 79,* 5412-5427, 1974.

Oxburgh, E.R., and E.M. Parmentier, Compositional and density

stratification in oceanic lithosphere-causes and consequences, *J. Geol. Soc. London, 133*, 343-355, 1977.

Pennington, W.D., Role of shallow phase changes in the subduction of oceanic crust, *Science, 220*, 1045-1047, 1983.

Purdy, G.M., The seismic structure of 140 Myr old crust in the western central Atlantic Ocean, *Geophys. J. Roy. Astron. Soc., 72*, 115-137, 1983.

Purdy, G.M. , and J. Ewing, Seismic structure of the ocean crust, *DNAG Synthesis*, vol. M, *The Western Atlantic Region*, pp. 313-330, Geological Society of America, Boulder, Colo., 1986.

Raitt, R.W., The crustal rocks, *The Sea*, vol.3, edited by M.N. Hill, pp. 84-102, Wiley, Interscience, New York, 1963.

Robinson, P.T., et al., *Proceedings of ODP, Initial Reports*, vol. *118*, Ocean Drilling Program, College Station, Tex., 1989.

Salisbury, M.H., and N.I. Christensen, The seismic velocity structure of a traverse through the Bay of Islands ophiolite complex, Newfoundland, an exposure of ocean crust and upper mantle, *J. Geophys. Res., 83*, 805-817, 1978.

Salisbury, M.H., R.,Stephen, N.I. Christensen, J. Francheteau, Y. Hamano, M. Hobart, and D. Johnson, The physical state of the upper levels of Cretaceous oceanic crust from the results of logging, laboratory studies and the oblique seismic experiment at DSDP sites 417 and 418, *Initial Rep. Deep Sea Drill. Proj., 51-53*, 113-134, 1980.

Salisbury, M.H., et al. *Proceedings of ODP, Initial Reports*, Vol. *102*, Ocean Drilling Program, College Station, Tex., 1986a.

Salisbury, M.H., et al., Old oceanic crust: Synthesis of logging, laboratory and seismic data from leg 102, *Proc. Ocean Drill. Program, Sci. Results, 102*, 155-180, 1988.

Salisbury, M.H., et al., *Proceedings of ODP, Scientific Results*, vol. *102*, Ocean Drilling Program, College Station, Tex., 1986b.

Shor, G.G., Jr., H.W. Menard and R.W. Raitt, Structure of the Pacific basin, *The Sea* vol. *4*, edited by Maxwell, A.E.., pp. 3-27, Wiley, Interscience New York, 1971.

Spudich, P., and J. Orcutt, A new look at the seismic velocity structure of the oceanic crust., *Rev. Geophys., 18*, 627-645, 1980.

Swift, S.A., R.A. Stephen, and H. Hoskins, Structure of upper oceanic crust from an oblique seismic experiment at hole 418A, western North atlantic, *Proc. Ocean Drill. Program, Sci. Results, 102*, 97-124, 1988.

Vera, E.E., and J.G. Mutter, Crustal structure in the Rose area of the East Pacific Rise: One-dimensional travel time inversion of sonobuoys and expanded spread profiles, *J. Geophys. Res., 93*, 6635-6648, 1988.

Watts, A.B., and M. Talwani, Gravity anomalies seaward of deep-sea trenches and their tectonic implications, *Geophys. J.Roy. Astron . Soc., 6*, 57-90, 1974.

Whitmarsh, R.B.. Seismic refraction studies of the upper igneous crust in the north Atlantic and porosity estimates from layer 2, *Earth Planet. Sci. Lett., 37*, 451-464. 1978.

Wilkens, R., D. Schultz, and R. Carlson, Relationship of resistivity, velocity, and porosity for basalts from downhole well-logging measurements in hole 418A, *Proc. Ocean Drill. Program, Sci. Results, 102*, 69-75, 1988.

R.L. Carlson and C.N. Herrick, Geodynamics Research Institute, Texas A&M University, College Station, TX 77843

(Received July 14, 1989;
revised November 10, 1989;
accepted November 12, 1989.)